Pollutants and insecticides drive local adaptation in African malaria mosquitoes

Colince Kamdem[1*], Caroline Fouet[1], Stephanie Gamez[1], Bradley J. White[1,2,*]

[1]Department of Entomology, University of California, Riverside, CA 92521

[2]Center for Disease Vector Research, Institute for Integrative Genome Biology, University of California, Riverside, CA 92521

[*]Corresponding author: e-mail: colincek@ucr.edu; bwhite@ucr.edu

ABSTRACT

The *Anopheles gambiae* complex contains a number of highly anthropophilic mosquito species that have acquired exceptional ability to thrive in complex human habitats. Thus, examining the evolutionary history of this Afrotropical mosquito may yield vital information on the selective processes that occurred during the adaptation to human-dominated environments. We performed reduced representation sequencing on 941 mosquitoes of the *Anopheles gambiae* complex collected across four ecogeographic zones in Cameroon. We find evidence for genetic and geographic subdivision within *An. coluzzii* and *An. gambiae* sensu *s*tricto – the two most significant malaria vectors in the region. Importantly, in both species, rural and urban populations are genetically differentiated. Genome scans reveal pervasive signatures of selection centered on genes involved in xenobiotic resistance. Notably, a selective sweep containing detoxification enzymes is prominent in urban mosquitoes that exploit polluted breeding sites. Overall, our study suggests that recent anthropogenic environmental modifications and widespread use of insecticides are driving population differentiation and local adaptation in vectors with potentially significant consequences for malaria epidemiology.

INTRODUCTION

Humans and their actions on ecosystems can profoundly alter the evolutionary trajectory of other organisms in various ways (Palumbi 2001; Bull and Maron 2016; Hendry et al. 2017). Signatures of human-driven evolutionary changes are particularly evident in cities and urbanizing regions, which often necessitate a rapid adaptation to complex environments (Alberti 2015; Alberti et al. 2017; Hendry et al. 2017). A wealth of data exists on genetic and phenotypic signals associated with adaptation to anthropogenic changes in multiple taxa, but the extent of signatures across genomes remain largely unexplored. The widespread use of xenobiotics in agriculture and public health also increases selective pressures on pathogens and their vectors, prompting significant evolutionary adjustments that have yet to be fully elucidated (Georghiou 1972; Mallet 1989; Palumbi 2001). The application of powerful genomic tools now available will help identify the genes and genomic regions underlying adaptation to human-induced selective pressures.

The most effective malaria mosquitoes of the Afrotropical region are remarkably anthropophilic and closely associated with human habitats (White 1974; Coluzzi et al. 1979; Antonio-Nkondjio et al. 2006; Sinka et al. 2010; Dia et al. 2013). Therefore, dissecting the genome of contemporary populations of these species may provide significant insights into the genetic targets of recent selection driven by anthropogenic disturbance. Adaptation to human-dominated environments is challenging and very selective even among highly specialized mosquitoes that feed almost exclusively on human hosts. For example, tens of

60 *Anopheles* species transmit human malaria parasites across the continent, but
61 only four members of the *Anopheles gambiae* complex thrive in dense urban
62 areas (Antonio-Nkondjio et al. 2005; Oyewole and Awolola 2006; Mourou et al.
63 2010; Dabiré et al. 2012; Kamdem et al. 2012). The recent scaling up of
64 measures using insecticides and insecticide-treated materials to combat malaria
65 expose mosquitoes to an even more disruptive adaptive challenge (Sokhna et al.
66 2013; WHO 2013). Although the genetic basis remains unknown, studies suggest
67 that both physiological and ecological limits and species ranges are profoundly
68 altered in *Anopheles* mosquitoes as a result of rapid urbanization and
69 widespread use of insecticides (Jones et al. 2012; Kamdem et al. 2012;
70 Mwangangi et al. 2013; Tene Fossog et al. 2013; Antonio-Nkondjio et al. 2015).

71 The *Anopheles gambiae* complex is a group of at least nine isomorphic
72 mosquito species exhibiting varying degrees of geographic and reproductive
73 isolation (Riehle et al. 2011; Coetzee et al. 2013; Fontaine et al. 2015). Owing to
74 ongoing adaptive speciation, the principal vectors of the complex have an
75 amazing plasticity in adjusting to diverse ecological conditions, allowing them to
76 track humans across most of tropical Africa (Davidson 1964; Coluzzi et al. 1979;
77 Coluzzi et al. 2002). This adaptive flexibility and the underlying behavioral
78 complexity have undermined at least one major effort at vector control
79 (Molineaux and Gramiccia 1980). Importantly, the epidemiological consequences
80 of adaptive radiation will be even more challenging to tackle if a part of the
81 divergence recently described within the particularly efficient vectors *An.*
82 *gambiae* sensu stricto (hereafter *An. gambiae*) and *An. coluzzii* is driven by

human-induced changes (Touré et al. 1998; Wondji et al. 2005; Slotman et al. 2007; Pinto et al. 2013; Caputo et al. 2014). This hypothesis has been formulated based on ecological observations and population structure, but the genetic underpinnings still need to be clearly assessed by examining patterns of variation across the genome (Coluzzi et al. 2002; Kamdem et al. 2012; Caputo et al. 2014).

To delineate the population structure and the role of recent processes – mainly urbanization and the rapid scaling up of insecticide-treated bed net coverage – in the genetic differentiation, we genotyped 941 mosquitoes of the *An. gambiae* complex collected from diverse environments in Cameroon at >8,000 SNP. We found strong evidence for complex geographic and genetic structuring giving rise to seven subpopulations distributed along a continuum of genomic differentiation within both *An. gambiae* and *An. coluzzii*. By combining genomic evidence and ecological knowledge, we revealed that the strongest correlates of genetic differentiation in this region are intense suburban agriculture, urbanization, insecticides and forest-savannah subdivisions. These findings add to a growing body of data indicating that the inevitable rise of insecticide resistance together with ongoing local adaptation of *Anopheles* species in urban areas are the major challenges for current vector control strategies.

RESULTS

Population structure of An. gambiae *sensu lato (s.l.) sibling species*

We performed extensive sampling of human-associated *Anopheles* across

106 the main ecological zones in Cameroon (Table S1, Figure S1) to collect diverse
107 populations belonging to the four species of the *An. gambiae* complex that are
108 known to occur in the country (Simard et al. 2009). Certain subpopulations or
109 species can be overlooked when sampling is biased toward one type of
110 population (Riehle et al. 2011). To maximize the chances that our samples best
111 represent the genetic diversity within each species, we used several sampling
112 methods (Service 1993) to collect both larvae and adult populations. In addition,
113 populations of *An. gambiae* and *An. coluzzii* segregate along urbanization
114 gradients, which seem to be the most important driver of ecological divergence in
115 the forest zone (Kamdem et al. 2012). To validate this hypothesis and to
116 investigate the genomic targets of local adaptation in urban environments, we
117 surveyed several neighborhoods representing the urban and suburban
118 ecosystems in the two biggest cities of the forest area: Douala and Yaoundé
119 (Figure S1).

120 To assess the genetic relatedness among individuals, we subjected all
121 941 mosquitoes that were morphologically identified as *An. gambiae* s.l. to
122 population genomic analysis. Individual mosquitoes were genotyped in parallel at
123 a dense panel of markers using double-digest restriction associated DNA
124 sequencing (ddRADseq), which enriches for a representative and reproducible
125 fraction of the genome that can be sequenced on the Illumina platform (Peterson
126 et al. 2012). After aligning ddRADseq reads to the *An. gambiae* reference
127 genome, we used STACKS (Catchen et al. 2011; Catchen et al. 2013) to identify
128 8,476 SNPs (~1 SNP every 30kb across the genome) within consensus RAD loci

129 present in more than 80% of individuals, and we inferred the population structure
130 based on these variations. First, we performed principal component analysis
131 (PCA) across all 941 individuals (Figure 1A). The top three components explain
132 28.4% of the total variance and group individuals into five main clusters.
133 Likewise, a neighbor-joining (NJ) tree, based on Euclidian distance of allele
134 frequencies, shows five distinct clades of mosquitoes (Figure 1B). We
135 hypothesized that these groups at least partially correspond to the four sibling
136 species – *An. gambiae*, *An. coluzzii*, *An. arabiensis*, and *An. melas* – known to
137 occur in Cameroon. To confirm, we typed a subset of 288 specimens using
138 species identification PCRs (Fanello et al. 2002; Santolamazza et al. 2004) and
139 found that each cluster comprised a single species. In agreement with previous
140 surveys (Wondji et al. 2005; Simard et al. 2009), our collections indicate that the
141 brackish water breeding *An. melas* is limited to coastal regions, while the arid-
142 adapted *An. arabiensis* is restricted to the savannah. In contrast, *An. gambiae*
143 and *An. coluzzii* are distributed across the four eco-geographic zones of
144 Cameroon (Figure 1D). Lee et al. 2013 recently reported frequent bouts of
145 hybridization between *An. gambiae* and *An. coluzzii* in Cameroon. While both the
146 PCA and NJ trees clearly separate the two species, the PCA does show
147 intermixing of some rare individuals consistent with semi-permeable species
148 boundaries.

149 In support of population structuring below the species level, Bayesian
150 clustering analysis with fastSTRUCTURE (Raj et al. 2014) finds that 7 population
151 clusters (*k*) best explain the genetic variance present in our data (Figure 1C,

152 Figure S2). Indeed, grouping of samples within *An. gambiae* and *An. coluzzii*
153 clades suggests that additional subdivision may exist within each species (Figure
154 1A, 1B). Ancestry plots further support inference from the PCA and NJ tree: at
155 least two subgroups compose *An. coluzzii* and *An. gambiae* individuals show
156 admixed ancestry, while *An. arabiensis* and *An. melas* are panmictic (Figure 1C,
157 Figure S2). A cryptic subgroup of *An. gambiae* has been discovered recently by
158 comparing indoor and outdoor fauna from the same village in Burkina Faso
159 (Riehle et al. 2011). Visual inspections of our PCA, NJ and fastSTRUCTURE
160 clustering results do not indicate any genetic subdivision based on the collection
161 methods or the developmental stage. To explicitly test for the effects of the
162 sampling methods and the geographic origin of samples on the genetic variance
163 among individuals, we applied a hierarchical Analysis of Molecular Variance
164 (AMOVA) (Excoffier et al. 1992), which confirmed the absence of genetic
165 structuring based on microhabitats or temporal segregations in both species. The
166 large majority of the genetic variation is attributable to differences among
167 individuals. While the geographic origin accounts for 13.2 % ($p < 0.001$) and
168 9.4% ($p < 0.001$) of the variance in *An. coluzzii* and *An. gambiae* respectively, the
169 effect of the types of sample is marginal and not significant.
170
171 *Population Structure within* An. gambiae
172 To further resolve the population structure within 357 *An. gambiae*
173 specimens, we performed population genetic analysis with a set of 9,345 filtered
174 SNPs. Using a combination of PCA, NJ trees, and ancestry assignment, we

175 consistently identify three distinct subgroups within *An. gambiae* (Figure 2, Figure
176 S2). The first and largest subgroup (termed *GAM1*) comprises the vast majority
177 of all *An. gambiae* specimens including individuals collected in all four eco-
178 geographic regions (Table S1). A total of 17 individuals make up a second small
179 subgroup (termed *GAM2*). Interestingly, individuals assigned to this cluster
180 include both larvae and adults collected in 3 different villages spread across 2
181 eco-geographic regions. In the absence of any obvious evidence of niche
182 differentiation between *GAM1* and *GAM2,* it is unclear what is driving and/or
183 maintaining divergence between the two sympatric subgroups. Specimens
184 collected from Nkolondom, a suburban neighborhood of Yaoundé where larval
185 sites associated with small-scale agricultural irrigation are common (Fossog
186 Tene et al. 2013; Nwane et al. 2013), form a genetically distinct third subgroup
187 (termed *Nkolondom*) that appears to be a locally-adapted ecotype.
188
189 *Population Structure within* An. coluzzii
190 To examine population structure within 521 *An. coluzzii* specimens, we
191 utilized 9,822 SNPs that passed stringent filtration. All analyses show a clear split
192 between individuals from the northern savannah region and the southern three
193 forested regions of Cameroon (Coastal, Forest, Forest-Savannah) (Figure 3A-C).
194 In principle, the north-south structuring could be caused solely by differences in
195 chromosome 2 inversion frequencies, which form a cline from near absence in
196 the humid south to fixation in the arid north (Simard et al. 2009; Fouet et al.
197 2012). However, we find SNPs from all five chromosomal arms consistently

198 separate northern and southern mosquitoes, indicating a substantial genome-
199 wide divergence between the two populations (Figure S3).

200 Southern populations of *An. coluzzii* were collected from three different
201 areas: Douala (the largest city of Cameroon), Yaoundé (the second largest city)
202 and the rural coastal region. PCA, NJ trees, and fastSTRUCTURE show clear
203 clustering of southern samples by collection site (Figure 3D-F). Mosquitoes from
204 Douala, situated on the coastal border, contain a mixture of urban and coastal
205 polymorphisms as illustrated by their intermediate position along PC3 (Figure
206 3D). Despite considerable geographic segregation, clusters are not fully discrete,
207 likely owing to substantial migration between the three sites. Taken together, the
208 data suggest a dynamic and ongoing process of local adaptation within southern
209 *An. coluzzii*. In contrast, no similar geographic clustering is observed in northern
210 populations (Figure S2, S4). Slight variations can be observed between genetic
211 clustering patterns suggested by different methods. We have only considered
212 subdivisions that were consistent across the three methods we employed. For
213 example, individuals from Yaoundé have been treated as a single subgroup,
214 although PCA showed that a few specimens were relatively detached from the
215 main cluster. This putative subdivision was not supported by the NJ tree and
216 fastSTRUCTURE analyses (Figure 3D-F). All populations described as "urban"
217 were collected from the most urbanized areas of the city, which are characterized
218 by a high frequency of built environments as described in Kamdem *et al*. 2012.
219

220 *Relationships Between Species and Subgroups*

221 Population genomic analysis identified four different *An. gambiae* s.l.
222 species present within our samples. Within *An. gambiae* and *An. coluzzii* we
223 identified seven potential subgroups with apparently varying levels of divergence.
224 To further explore the relationships between different populations, we built an
225 unrooted NJ tree using pairwise levels of genomic divergence (F_{ST}) between all
226 species and subgroups (Figure 4, Table S2). As previously observed in a
227 phylogeny based on whole genome sequencing (Fontaine et al. 2015), we find
228 that *An. melas* is highly divergent from all other species (F_{ST} ~ 0.8), while *An.*
229 *arabiensis* shows intermediate levels of divergence (F_{ST} ~ 0.4) from *An. gambiae*
230 and *An. coluzzii*. As expected, the sister species *An. gambiae* and *An. coluzzii*
231 are more closely related to each other (F_{ST} ~ 0.2) than any other species. When
232 examining differentiation between subgroups within *An. coluzzii*, we find that the
233 southern and northern subgroups are relatively divergent (F_{ST} > 0.1), while
234 differentiation between local ecotypes within the south is much lower (F_{ST} <
235 0.04), corroborating patterns of population structure described within this species
236 (Figure 3D-F). Similarly, as suggested by the genetic structuring, the level of
237 differentiation between *An. gambiae* subgroups *GAM1* and *GAM2* is relatively
238 significant (F_{ST} ~ 0.1), while the suburban ecotype from Nkolondom shows a low
239 level of divergence from *GAM1* (F_{ST} ~ 0.05). To further examine the degree of
240 isolation of subgroups within species, we assessed the reductions in observed
241 heterozygosity with respect to that expected under Hardy–Weinberg Equilibrium
242 among *An. coluzzii* and *An. gambiae* populations, by computing the average
243 Wright's inbreeding coefficient, F_{IS}, across genome-wide SNPs. Values of F_{IS}

244 close to 1 indicate a deviation from Hardy–Weinberg Equilibrium and the
245 existence of cryptic subdivisions while F_{IS} close to 0 suggest that there are no
246 barriers to gene flow. In spite of the strong population genetic structure observed
247 within *An. coluzzii* and *An. gambiae*, we found surprisingly low genome-wide F_{IS}
248 values (less than 0.0003) in both species, suggesting a lack of assortative
249 mating. Overall, there is no evidence for reproductive isolation within *An.*
250 *gambiae* and *An. coluzzii* despite ongoing local adaptation and significant
251 population differentiation.
252
253 *Signatures of selection*
254 To find potential targets of selection within subgroups, we performed
255 scans of nucleotide diversity (θ_w, θ_π) and allele frequency spectrum (*Tajima's D*)
256 in non-overlapping 150-kb windows across the genome. Scans of θ_w, θ_π, *and*
257 *Tajima's* D were conducted by importing aligned, but otherwise unfiltered, reads
258 directly into ANGSD, which uses genotype likelihoods to calculate summary
259 statistics (Korneliussen et al. 2014). Natural selection can increase the frequency
260 of an adaptive variant within a population, leading to localized reductions in
261 genetic diversity as the haplotype containing the adaptive variant(s) sweeps
262 towards fixation (Maynard Smith and Haigh 1974; Tajima 1989). Selective
263 processes can also promote the coexistence of multiple alleles in the gene pool
264 of a population (balancing selection). Thus, genomic regions harboring targets of
265 selection should exhibit extreme values of diversity and allele frequency spectra
266 relative to genome-wide averages (Storz 2005).

267 We also performed genome scans using both a relative (F_{ST}) and absolute
268 (d_{xy}) measure of divergence calculated with STACKS and *ngsTools* (Fumagalli et
269 al. 2014), respectively. For both diversity and divergence scans we used a
270 maximum of 40 mosquitoes per population, prioritizing individuals with the
271 highest coverage in populations when sample size exceeded 40. In contrast to
272 Tajima's *D* and F_{ST}, the genome-wide distribution of d_{xy} and nucleotide diversity
273 in 150-kb sliding windows yielded relatively noisy patterns due to a large variance
274 (Wakeley 1996) (Figure 5 and 6). As a result, the identification of signatures of
275 selection was based primarily on outliers of Tajima's *D* and F_{ST}. Estimates of d_{xy}
276 and nucleotide diversity were used to confirm genomic locations that were
277 pinpointed as candidate selective sweep on the basis of values of Tajima's *D* and
278 F_{ST}. Precisely, genomic regions were considered as targets of selection if they
279 mapped to significant peaks or depressions of diversity and d_{xy}, and their values
280 of F_{ST} and Tajima's *D* were among the top 1% of the empirical distribution in at
281 least one population. Significantly negative values of Tajima's *D* relative to the
282 genome-wide average suggest an increase in low-frequency mutations due to
283 negative or positive selection whereas significantly positive values of Tajima's *D*
284 indicate a balancing selection.
285
286 *Targets of Selection within* An. gambiae *subgroups*
287 Our estimates of genome-wide diversity levels (Table S3) within *An.*
288 *gambiae* subgroups are comparable to previous values based on RAD
289 sequencing of East African *An. gambiae* s.l. populations (O'Loughlin et al. 2014).

290 As expected, the large *GAM1* population harbors more genetic diversity than the
291 apparently rare *GAM2* population or the geographically restricted Nkolondom
292 ecotype (Table S3, Figure 5A-C). *Tajima's D* is consistently negative across the
293 entire genome of all three subgroups, indicating an excess of low-frequency
294 variants that are likely the result of recent population expansion (Figure 5A-C).
295 Indeed, demographic models infer relatively recent bouts of population expansion
296 in all three subgroups (Table S4).

297 Genome scans of each subgroup reveal genomic regions that show
298 concordant reductions in diversity and allele frequency spectrum consistent with
299 selection (highlighted in Figure 5 A-C). Based on the 1% cutoff of Tajima's *D*
300 (upper and lower bounds) and F_{ST}, we identified 4 candidate regions exhibiting
301 strong signatures of selection. It should be noted that due to the reduced
302 representation sequencing approach we used, our analysis may be highlighting
303 only clear instances of selection, which are likely both recent and strong (Tiffin
304 and Ross-Ibarra 2014). An apparent selective event on the left arm of
305 chromosome 2 near the centromere is found in all populations. This selective
306 sweep is characterized by a prominent depression of Tajima's *D* (~1.5Mb in
307 width) and contains ~80 genes including the pyrethroid knockdown resistance
308 gene (*kdr*). Although it is difficult to precisely identify the specific gene that has
309 been influenced by selection in this region, the voltage-gated sodium channel
310 gene (*kdr*), which is a pervasive target of selection in *Anopheles* mosquitoes
311 (Clarkson et al. 2014; Norris et al. 2015) represents the strongest candidate in
312 our populations. Three mutations of the para-type sodium channel conferring

313 knockdown resistance (1014F, 1014L and 1014S) are widespread in Cameroon
314 (Nwane et al. 2011). The drop in Tajima's *D* in the putative *kdr* sweep is sharpest
315 in the Nkolondom population. Both 1014F and 1014L *kdr* alleles coexist at high
316 frequencies in mosquitoes from this suburban neighborhood of Yaoundé where
317 larvae can be readily collected from irrigated garden plots that likely contain
318 elevated levels of pesticides directed at agricultural pests (Nwane et al. 2011;
319 Fossog Tene et al. 2013; Nwane et al. 2013).

320 Another region exhibiting consistent signatures of selection in all
321 populations is found around the centromere on the X chromosome. Functional
322 analyses of gene ontology (GO) terms (Table S5) revealed a significant
323 representation of chitin binding proteins in this sweep (p = 1.91e-4). A strong
324 genetic divergence among the three subgroups of *An. gambiae* characterized by
325 significant F_{ST} and d_{xy} peaks is also observed at ~30 Mb and ~40 Mb on
326 chromosome 3R. Positive outliers of both Tajima's *D* and nucleotide diversity
327 suggest that this genetic divergence is due to balancing selection on multiple
328 alleles among populations. Functional analyses of GO terms indicate that the
329 region at ~40 Mb on 3R is enriched in cell membrane proteins, genes involved in
330 olfaction and epidermal growth factors (EGF) genes (Table S5). Finally, a striking
331 depression in Tajima's *D* supported by a marked dip in nucleotide diversity
332 occurs on chromosome 2L from ~33-35 Mb in the Nkolondom population
333 exclusively (Figure 5A-C). Despite the lack of genetic differentiation, this region –
334 enriched in six EGFs (Table S5) – is probably a recent selective sweep, which

335 could facilitate larval development of this subgroup in pesticide-laced agricultural
336 water.
337
338 *Targets of Selection within* An. coluzzii *subpopulations*
339 As above, we used diversity, allele frequency spectra and genetic
340 differentiation metrics to scan for targets of selection in the four subgroups of *An.*
341 *coluzzii*. Overall, genetic diversity is higher in the northern savannah population
342 than either of three southern populations, which all exhibit similar levels of
343 diversity (Table S3). Just as in *An. gambiae*, all subgroups have consistently
344 negative Tajima's *D* values confirming demographic models of population
345 expansion (Table S4).
346 We detected 33 regions where either F_{ST} or Tajima's *D* was above the 99th
347 percentile of the empirical distribution in at least one population. This included at
348 least 10 hotspots of F_{ST} clustered within the 2L*a* inversion, which segregates
349 between forest and savannah populations, as well as a region centered on the
350 resistance to dieldrin (*rdl*) locus at ~25 Mb on 2L (Figure 6H). However, based on
351 the 1% threshold of both Tajima's *D* and F_{ST}, we found only 5 candidate selective
352 sweeps including the *kdr* region, the sweep on the X chromosome, and the two
353 hot spots of balancing selection detected on the chromosome 3R in *An. gambiae*
354 (Figure 6A-D). The fifth putative selective sweep characterized by a sharp drop in
355 both diversity and Tajima's *D* occurs on 3R from ~28.5-29.0 Mb, with the decline
356 being more significant in urban populations. The particularly reduced diversity at
357 this sweep in urban mosquitoes strongly suggests it may contain variant(s) that

358 confer adaptation to human-induced changes. Indeed, this genomic region
359 harbors a cluster of both Glutathione S-transferase (*GSTE1-GSTE7*) and
360 cytochrome P450 (*CYP4C27*, *CYP4C35*, *CYP4C36*) genes, and functional
361 analyses of GO terms reveals an overrepresentation of terms containing
362 "Glutathione S-transferase" (Table S5, p = 5.14e-10). Both the *GSTE* and
363 cytochrome P450 gene families are known to confer metabolic resistance to
364 insecticides and pollutants in mosquitoes (Enayati et al. 2005; David et al. 2013).
365 In particular, *GSTE5* and *GSTE6* are intriguing candidate targets of selection as
366 each is up-regulated in highly insecticide resistant *An. arabiensis* populations that
367 recently colonized urban areas of Bobo-Dioulasso, Burkina Faso (Jones et al.
368 2012).

369 Both relative and absolute divergences between populations at the two
370 selective sweeps involved in xenobiotic resistance probably reflect a spatial
371 variation in selection along gradients of anthropogenic disturbance. In particular,
372 the *kdr* locus exhibits minimal divergence in all pairwise comparisons, suggesting
373 that the same resistance haplotype is under selection in each population (Figure
374 6E-H). This hypothesis is corroborated by data on the distribution of *kdr*
375 mutations in Cameroon (Nwane et al. 2011). As opposed to *An. gambiae*
376 populations, which are broadly polymorphic for three *kdr* alleles, the 1014L
377 mutation is the major allele present at very high frequencies in *An. coluzzii*
378 throughout the country. The GSTE/CYP450 sweep on 3R shows a peak in F_{ST},
379 but surprisingly low absolute divergence between Yaoundé and Coastal
380 mosquitoes – a pattern consistent with genomic regions that underwent a

381 selective sweep over a broad geographic area followed by episodes of within-
382 population selection leading to reduced diversity across certain locations (Irwin et
383 al. 2016). Comparisons between Douala and Coastal populations show a more
384 moderate increase in F_{ST}, presumably due to high rates of migration between
385 these nearby sites. To further explore the 3R GSTE/CYP450 sweep, we
386 reconstructed haplotypes for all 240 *An. coluzzii* southern chromosomes across
387 the 28 SNPs found within the sweep. In the Yaoundé population, a single
388 haplotype is present on 44 out of 80 (55%) chromosomes (all grey SNPs), while
389 an additional 11 haplotypes are within one mutational step of this common
390 haplotype (Figure 7A). In Douala, the same haplotype is the most common, but
391 present at a lower frequency (31%) than in Yaoundé (Figure 7B). This haplotype
392 is found on only 6/80 (7.5%) coastal chromosomes (Figure 7C). Population
393 genomic analyses of the same 28 SNPs (Figure 7D-F) mirror results of the
394 haplotype analysis, confirming that haplotype inference did not bias the results.
395

DISCUSSION

Genetic differentiation within species of the An. gambiae *complex*

The *An. gambiae* complex is a model of adaptive radiation with a puzzling evolutionary history (Coluzzi et al. 2002; Ayala and Coluzzi 2005). Due to the lack of observable phenotypes that segregate between populations, it is almost impossible to tackle the genetic basis of divergence between and within species of the complex using traditional genetic mapping methods. Consequently, the examination of sequence divergence in the wild with high-throughput sequencing and genotyping approaches is particularly adapted to address the environmental and genomic targets of ecological divergence in *An. gambiae* s.l. In that respect, patterns of genomic divergence have started to be dissected and significant insights have been gained into the signatures of selection among continental populations (Lawniczak et al. 2010; Neafsey et al. 2010; White et al. 2011). However, ecological divergence and local adaptation within species of the *An. gambiae* complex sometimes occur at lower spatial scales (often a few kilometres) (Sogoba et al. 2008; Kamdem et al. 2012) that are ignored by continental-scale analyses. Here we have applied a population genomic approach to investigate the genomic architecture of selection across a more restricted geographic area characterized by a great environmental diversity. We first showed that reduced representation sequencing of 941 *An. gambiae* s.l. collected in or near human settlements in 33 sites scattered across Cameroon facilitated rapid identification of known sibling species and revealed a complex hierarchical population structure within *An. gambiae* and *An. coluzzii*. This result

419 is opposite to that found in East Africa, where RADseq markers detected no
420 population differentiation within species of the *An. gambiae* complex (O'Loughlin
421 et al. 2014). Indeed, contrary to their East African counterparts, West African
422 populations have a long history of genetic differentiation that is still unresolved
423 despite the application of several generations of genetic markers (Coluzzi et al.
424 1979; Touré et al. 1998; Coluzzi et al. 2002; Wondji et al. 2002). Polymorphic
425 chromosomal inversions and microsatellite markers have suggested the
426 presence of additional subdivision within *An. coluzzii* in Cameroon (Wondji et al.
427 2005; Slotman et al. 2007). Using genome-wide SNPs, we have shown that this
428 subdivision results in at least three genetically distinct clusters including
429 populations from the savannah, coastal and urban areas. Little is known about
430 the phenotypic differentiation of these populations, but recent studies suggest
431 that mosquitoes from the coastal region tolerate higher concentrations of salt
432 (Tene Fossog et al. 2015) while urban populations are highly resistant to
433 insecticides and environmental pollutants (Antonio-Nkondjio et al. 2011; Fossog
434 Tene et al. 2013; Tene Fossog et al. 2013; Antonio-Nkondjio et al. 2015). Models
435 of ecological niches of *An. gambiae* s.l. in Cameroon predict that favourable
436 habitats of *An. coluzzii* populations are fragmented and marginal in contrast to
437 *An. gambiae*, which occupies a broad range across the country (Simard et al.
438 2009). In line with this prediction, we have found a weak differentiation and
439 higher diversity in *An. gambiae* over significant geographic areas despite the
440 presence of an emerging suburban cluster in Nkolondom.
441

442 *Genomic signatures of selection*

443 When approached with powerful tools, sensitive enough to capture
444 shallow and recent processes, populations depicting increasing levels of genetic
445 differentiation along a speciation continuum may provide insights into the targets
446 of selection at early stages of ecological divergence (Savolainen et al. 2013). In
447 principle, weakly differentiated populations such as the subgroups we described
448 typically display a marginal genomic divergence because there has not been
449 enough time for neutral and selective forces to shape the genomic architecture
450 (Nosil and Feder 2012; Andrew and Rieseberg 2013). Indeed, we found
451 signatures consistent with selection only across a handful of loci in structured
452 populations of *An. gambiae* and *An. coluzzii*. Although some targets of selection
453 are likely missing due to the limited genomic coverage of the RADseq approach
454 we used (Arnold et al. 2013; Tiffin and Ross-Ibarra 2014), the few selective
455 sweeps we found are relevant based on the genes they contain. Specifically, the
456 five main targets of selection in our populations are enriched in genes whose
457 functions include insecticide resistance and detoxification, epidermal growth,
458 cuticle formation and olfaction. The cuticle plays a major role at the interface
459 between several biological functions in insects and recent data support the
460 hypothesis that the coevolution of multiple mechanisms, including cuticular
461 barriers, has occurred in highly pyrethroid-resistant *An*. *gambiae* (Balabanidou et
462 al. 2016). Olfaction also mediates a wide range of both adult and larval
463 behaviours including feeding, host preference, and mate selection in blood-
464 feeding insects (Bowen 1991; Carey et al. 2010; Takken and Verhulst 2013).

465 Finally, due to the extreme association between the most effective vectors of the
466 *An. gambiae* complex and human habitats, a long-standing hypothesis has
467 suggested that human-driven selection is the main modulator of ecological
468 divergence between and within species (Coluzzi et al. 1979; Coluzzi et al. 2002;
469 Kamdem et al. 2012; Caputo et al. 2014). Consistent with this hypothesis, we
470 have found that urban and suburban mosquitoes are genetically differentiated
471 from rural populations and exhibit strong signatures of recent selection at loci
472 containing xenobiotic resistance genes.

473 *Anopheles* mosquitoes currently experience strong selective pressures
474 across the African continent due to the increased use of pesticides/insecticides in
475 agriculture and vector control over the last few decades (WHO 2012; Reid and
476 McKenzie 2016). The idea that insecticide resistance can affect the population
477 structure of mosquitoes as a result of a limited gene flow and/or local adaptation
478 between resistant and sensitive populations was already evoked in the 1990s
479 (Silvestrini et al. 1998; Lenormand et al. 1999). In addition to increased
480 resistance, large-scale exposure of vector populations to insecticide-treated bed
481 nets in Africa is also correlated with changes in species distribution and
482 behavioral shifts (Bøgh et al. 1998; Derua et al. 2012; Moiroux et al. 2012;
483 Mwangangi et al. 2013; Sokhna et al. 2013). However, so far, there is no
484 evidence that these changes can lead to genetic clustering or the creation of
485 cryptic populations within species (Main et al. 2016). Our data also support that
486 the genetic differentiation within the *An. gambiae* complex in Cameroon is due to
487 regional-scale subdivisions that do not correspond to known distributional or

488 behavioural shifts. Previous studies have documented significant reductions in
489 the population size of *An. gambiae* s.l. after introduction of long lasting
490 insecticide treated nets, but did not determine the influence of exposure on
491 population or genomic structuring (Athrey et al. 2012). The demographic history
492 of subgroups of *An. gambiae* and *An. coluzzii* inferred from allele frequency
493 spectra does not indicate signals of recent population bottlenecks that can be
494 associated with insecticide exposure (supplementary information, Table S4). It
495 has also been shown that adaptive introgression, allowing genomic regions
496 containing insecticide resistance genes to spread among sibling species of *An.*
497 *gambiae* s.l., coincides with major insecticide-treated net distribution campaigns
498 (Clarkson et al. 2014; Norris et al. 2015). Although the frequency of natural
499 hybrids is low (less than 2%), episodic gene flow occurs between species of the
500 complex in Cameroon (Lee et al. 2013), but adaptive introgression at insecticide
501 resistance loci have yet to be explicitly demonstrated in this region. Insecticide
502 resistance, involving both multiple alleles of *kdr* and significant levels of
503 metabolic resistance, is widespread among *An. gambiae* and *An. coluzzii*
504 populations in Cameroon especially in urban areas and locations where intensive
505 farming practices are common (Ndjemaï et al. 2009; Antonio-Nkondjio et al.
506 2011; Nwane et al. 2011; Fossog Tene et al. 2013; Nwane et al. 2013; Antonio-
507 Nkondjio et al. 2015). Alongside a mass distribution of insecticide-treated nets
508 throughout the country that was held in 2011, indoor residual insecticide spraying
509 has been tested in a few pilot locations, but this approach is not yet applied on a
510 large scale (Etang et al. 2011; Bowen 2013). We hypothesized that regional

511 variations in insecticide exposure exist across the country and contribute to the
512 patterns observed at the two selective sweeps associated with xenobiotic
513 resistance. Knockdown and metabolic resistance involving some of the genes
514 present in the 3R GSTE/CYP450 sweep are the most common resistance
515 mechanisms against the classes of insecticides currently used on a large scale
516 that are found in *An. gambiae* s.l (Nwane et al. 2013). As expected, urban and
517 suburban populations that are exposed to higher levels of insecticides/pollutants
518 exhibit stronger signals of selection (Kamdem et al. 2012; Fossog Tene et al.
519 2013; Tene Fossog et al. 2013). Indeed, the synergistic effects of the two types
520 of xenobiotics could be exerting intense selection pressure for pleiotropic
521 resistance in urban mosquitoes (Nwane et al. 2013). Further analysis of the 3R
522 GSTE/CYP450 sweep using a combination of whole genome resequencing and
523 functional genomic approaches should help resolve the specific genes that are
524 targets of local adaptation in this region of the genome. Additional studies are
525 also needed to further characterize the spatial and temporal variations as well as
526 the haplotypes correlated with insecticide-induced selection within the sweeps.

527 Effective strategies for managing insecticide resistance that has reached a
528 critical tipping point among malaria vectors on the continent are urgently needed
529 (Hemingway et al. 2016; Ranson and Lissenden 2016). In addition, considerable
530 evidence suggests that insecticide resistance has much deeper consequences
531 on the mosquito biology by interfering with other key biological functions such as
532 the immune system, which in turn profoundly affects the fitness of the vector and
533 its efficiency to transmit the pathogen (vectorial capacity) (Alout et al. 2013; Alout

534 et al. 2014; Alout et al. 2016). As a result, detailed knowledge of genomic
535 signatures of insecticide resistance and their pleiotropic effects on vectorial
536 capacity is necessary to design effective resistance management. Surprisingly,
537 despite intense research on insecticide resistance, this information is lacking in
538 all malaria vectors partly because efforts have so far focused on a few resistance
539 genes and have failed to capture the widespread effects of insecticide resistance
540 across the genome. The population genomic approaches we have used are
541 among the new tools that are being applied to investigate the genomic targets of
542 insecticide resistance at a fine scale in mosquitoes and will facilitate the
543 development of rational resistance management strategies.
544

545 *MATERIALS AND METHODS*

546

547 *Mosquito collections*

548 We collected *Anopheles* mosquitoes from 33 locations spread across the
549 four major ecogeographic regions of Cameroon from August to November 2013
550 (Table S1). All collections were performed by researchers who were given
551 malaria prophylaxis before and after the collection period. Indoor resting adult
552 mosquitoes were collected by pyrethrum spray catch, while host-seeking adults
553 were obtained via indoor/outdoor human-baited landing catch. Larvae were
554 sampled using standard dipping procedures (Service 1993). Individual
555 mosquitoes belonging to the *An. gambiae* complex were identified using
556 morphological keys (Gillies and De Meillon 1968; Gillies and Coetzee 1987).

557

558 *ddRADseq Library Construction*

559 Genomic DNA was extracted from adults using the ZR-96 Quick-gDNA kit
560 (Zymo Research) and from larvae using the DNeasy Extraction kit (Qiagen). A
561 subset of individuals were assigned to sibling species using PCR-RFLP assays
562 that type fixed SNP differences in the rDNA (Fanello et al. 2002; Santolamazza
563 et al. 2004). Preparation of ddRAD libraries largely followed (Turissini et al.
564 2014). Briefly, ~1/3rd of the DNA extracted from an individual mosquito (10µl) was
565 digested with *MluC1* and *NlaIII* (New England Biolabs). Barcoded adapters (1 of
566 48) were ligated to overhangs and 400 bp fragments were selected using 1.5%
567 gels on a BluePippin (Sage Science). One of six indices was added during PCR

568 amplification. Each library contained 288 individuals and was subjected to single
569 end, 100 bp sequencing across one or two flow cells lanes run on an Illumina
570 HiSeq2500.

571 Raw sequence reads were demultiplexed and quality filtered using the
572 STACKS v 1.29 process_radtags pipeline (Catchen et al. 2011; Catchen et al.
573 2013). After removal of reads with ambiguous barcodes, incorrect restriction
574 sites, and low sequencing quality (mean Phred < 33), GSNAP (Wu and Nacu
575 2010) was used to align reads to the *An. gambiae* PEST reference genome
576 (AgamP3) allowing up to five mismatches per read. The STACKS pipeline was
577 then used to identify unique RAD tags and construct consensus assemblies for
578 each and to call individual SNP genotypes using a maximum-likelihood statistical
579 model.

580

581 *Population Genomic Analysis*

582 Population genetic structure was assessed using the SNP dataset output
583 by the *populations* program of STACKS. We used PLINK v 1.19 to retrieve
584 subsets of genome-wide SNPs as needed (Purcell et al. 2007). PCA, neighbor-
585 joining tree analyses, and Bayesian information criterion (BIC) were implemented
586 using the packages *adegenet* and *ape* in R (Paradis et al. 2004; Jombart 2008; R
587 Development Core Team 2014). Ancestry analyses were conducted in
588 fastSTRUCTURE v 1.0 (Raj et al. 2014) using the logistic method. The
589 choosek.py script was used to find the appropriate number of populations (k); in
590 cases where a range of k was suggested, the BIC-inferred number of clusters

591 was chosen. CLUMPP v1.1.2 (Jakobsson and Rosenberg 2007) was used to
592 summarize assignment results across independent runs and DISTRUCT v1.1
593 (Rosenberg 2004) was used to visualize ancestry assignment of individual
594 mosquitoes. We used a subset of 1,000 randomly chosen SNPs to calculate
595 average pairwise F_{ST} between populations in GENODIVE v 2.0 using up to 40
596 individuals – prioritized by coverage – per population (Meirmans and Van
597 Tienderen 2004). Using this same subset of 1,000 SNPs, we conducted an
598 AMOVA (Excoffier et al. 1992) to quantify the effect of the sampling method and
599 the geographic origin on the genetic variance among individuals in GENODIVE.
600 We used 10,000 permutations to assess significance of F_{ST} values and AMOVA.
601 We input pairwise F_{ST} values into the program Fitch from the Phylip (Plotree and
602 Plotgram 1989) suite to create the population-level NJ tree. F_{IS} values were
603 computed with the *populations* program in STACKS.
604
605 *Genome Scans for Selection*
606 We used ANGSD v 0.612 (Korneliussen et al. 2014) to calculate
607 nucleotide diversity (θ_w and θ_π) and Tajima's *D* in 150-kb non-overlapping
608 windows. Unlike most genotyping algorithms, ANGSD does not perform hard
609 SNP calls, instead taking genotyping uncertainty into account when calculating
610 summary statistics. Similarly, absolute divergence (d_{xy}) was calculated using
611 *ngsTools* (Fumagalli et al. 2014) based on genotype likelihoods generated by
612 ANGSD. Kernel smoothed values for 150-kb windows for all four metrics (θ_w, θ_π,
613 *D*, d_{xy}) were obtained with the R package *KernSmooth*. F_{ST} (based on AMOVA)

614 was calculated with the *populations* program in STACKS using only loci present
615 in 80% of individuals. A Kernel smoothing procedure implemented in STACKS
616 was used to obtain F_{ST} values across 150-kb windows. Because regions with
617 unusually high or low read depth can yield unreliable estimates of diversity and
618 divergence parameters due to the likelihood of repeats and local misassembly,
619 we checked that the average per-locus sequencing coverage was consistent
620 throughout the genome (Figure S5). To determine if selective sweeps were
621 enriched for specific functional annotation classes, we used the program DAVID
622 6.7 with default settings (Huang et al. 2009). We delimitated the physical limits of
623 the selective sweep as the region corresponding to the base of the peak or the
624 depression of Tajima's *D*. Haplotypes across the GSTE/CYP450 sweep were
625 reconstructed by PHASE v 2.1.1 using the default recombination model
626 (Stephens et al. 2001; Stephens and Scheet 2005).
627

ACKNOWLEDGEMENTS

This work was supported by the University of California Riverside and National Institutes of Health (1R01AI113248, 1R21AI115271 to BJW). We thank Elysée Nchoutpouem and Raymond Fokom for assistance collecting mosquitoes and Sina Hananian for assisting in DNA extraction. We thank the editor and three anonymous reviewers for their constructive comments, which helped us to improve the manuscript. This work would not have been possible without the collaboration of inhabitants and administrative authorities of all sampled sites and we want to underscore their generosity and patience.

AUTHOR CONTRIBUTIONS

Conceived and designed the experiments: CK BJW. Performed the experiments: CK BJW SG. Analyzed the data: CK CF BJW. Wrote the paper: CK CF BJW.

643 REFERENCES

644 Alberti M. 2015. Eco-evolutionary dynamics in an urbanizing planet. Trends Ecol.
645 Evol. 30:114–126.

646 Alberti M, Marzluff J, Hunt VM. 2017. Urban driven phenotypic changes:
647 empirical observations and theoretical implications for eco-evolutionary
648 feedback. Philos. Trans. R. Soc. B Biol. Sci. 372:20160029.

649 Alout H, Dabiré RK, Djogbénou L, Abate L, Corbel V, Chandre F, Cohuet A.
650 2016. Interactive cost of *Plasmodium* infection and insecticide resistance in
651 the malaria vector *Anopheles gambiae*. Sci. Rep.:1–11.

652 Alout H, Djègbè I, Chandre F, Djogbénou LS, Dabiré RK, Corbel V, Cohuet A.
653 2014. Insecticide exposure impacts vector– parasite interactions in
654 insecticide- resistant malaria vectors. Proc. R. Soc. B Biol. Sci.
655 281:20140389.

656 Alout H, Ndam NT, Sandeu MM, Djégbe I, Chandre F, Dabiré RK, Djogbénou LS,
657 Corbel V, Cohuet A. 2013. Insecticide Resistance Alleles Affect Vector
658 Competence of Anopheles gambiae s.s. for Plasmodium falciparum Field
659 Isolates. PLoS One 8.

660 Andrew RL, Rieseberg LH. 2013. Divergence is focused on few genomic regions
661 early in speciation: incipient speciation of sunflower ecotypes. Evolution
662 67:2468–2482.

663 Antonio-Nkondjio C, Fossog BT, Ndo C, Djantio BM, Togouet SZ, Awono-
664 Ambene P, Costantini C, Wondji CS, Ranson H. 2011. Anopheles gambiae

665 distribution and insecticide resistance in the cities of Douala and Yaoundé
666 (Cameroon): influence of urban agriculture and pollution. Malar. J. 10:154.

667 Antonio-Nkondjio C, Kerah CH, Simard F, Awono-Ambene P, Chouaibou M,
668 Tchuinkam T, Fontenille D. 2006. Complexity of the malaria vectorial system
669 in Cameroon: contribution of secondary vectors to malaria transmission. J.
670 Med. Entomol. 43:1215–1221.

671 Antonio-Nkondjio C, Simard F, Awono-Ambene P, Ngassam P, Toto JC,
672 Tchuinkam T, Fontenille D. 2005. Malaria vectors and urbanization in the
673 equatorial forest region of south Cameroon. Trans. R. Soc. Trop. Med. Hyg.
674 99:347–354.

675 Antonio-Nkondjio C, Tene Fossog B, Kopya E, Poumachu Y, Menze Djantio B,
676 Ndo C, Tchuinkam T, Awono-Ambene P, Wondji CS. 2015. Rapid evolution
677 of pyrethroid resistance prevalence in Anopheles gambiae populations from
678 the cities of Douala and Yaoundé (Cameroon). Malar. J. 14.

679 Arnold B, Corbett-Detig RB, Hartl D, Bomblies K. 2013. RADseq underestimates
680 diversity and introduces genealogical biases due to nonrandom haplotype
681 sampling. Mol. Ecol. 22:3179–3190.

682 Athrey G, Hodges TK, Reddy MR, Overgaard HJ, Matias A, Ridl FC,
683 Kleinschmidt I, Caccone A, Slotman M a. 2012. The effective population size
684 of malaria mosquitoes: large impact of vector control. PLoS Genet.
685 8:e1003097.

686 Ayala FJ, Coluzzi M. 2005. Chromosome speciation: humans, Drosophila, and

687 mosquitoes. Proc. Natl. Acad. Sci. U. S. A. 102 Suppl:6535–6542.

688 Balabanidou V, Kampouraki A, MacLean M, Blomquist GJ, Tittiger C, Juárez MP,
689 Mijailovsky SJ, Chalepakis G, Anthousi A, Lynd A, et al. 2016. Cytochrome
690 P450 associated with insecticide resistance catalyzes cuticular hydrocarbon
691 production in *Anopheles gambiae*. Proc. Natl. Acad. Sci. 113:201608295.

692 Bøgh C, Pedersen EM, Mukoko D a, Ouma JH. 1998. Permethrin-impregnated
693 bednet effects on resting and feeding behaviour of lymphatic filariasis vector
694 mosquitoes in Kenya. Med. Vet. Entomol. 12:52–59.

695 Bowen HL. 2013. Impact of a mass media campaign on bed net use in
696 Cameroon. Malar. J. 12:36.

697 Bowen MF. 1991. The sensory physiology of host-seeking behavior in
698 mosquitoes. Annu. Rev. Entomol. 36:139–158.

699 Bull JW, Maron M. 2016. How humans drive speciation as well as extinction.
700 Proc. R. Soc. B 283:1–10.

701 Caputo B, Nwakanma D, Caputo FP, Jawara M, Oriero EC, Hamid-Adiamoh M,
702 Dia I, Konate L, Petrarca V, Pinto J, et al. 2014. Prominent intraspecific
703 genetic divergence within Anopheles gambiae sibling species triggered by
704 habitat discontinuities across a riverine landscape. Mol. Ecol. 23:4574–4589.

705 Carey AF, Wang G, Su CY, Zwiebel LJ, Carlson JR. 2010. Odorant reception in
706 the malaria mosquito Anopheles gambiae. Nature 464:66–71.

707 Catchen J, Hohenlohe P a., Bassham S, Amores A, Cresko W. 2013. Stacks: An
708 analysis tool set for population genomics. Mol. Ecol. 22:3124–3140.

709 Catchen JM, Amores A, Hohenlohe P, Cresko W, Postlethwait JH. 2011. Stacks:
710 building and genotyping Loci de novo from short-read sequences. G3
711 (Bethesda). 1:171–182.

712 Clarkson CS, Weetman D, Essandoh J, Yawson AE, Maslen G, Manske M, Field
713 SG, Webster M, Antão T, MacInnis B, et al. 2014. Adaptive introgression
714 between Anopheles sibling species eliminates a major genomic island but
715 not reproductive isolation. Nat. Commun. 5:4248.

716 Coetzee M, Hunt RH, Wilkerson R, Torre A Della, Coulibaly MB, Besansky NJ.
717 2013. Anopheles coluzzii and Anopheles amharicus, new members of the
718 Anopheles gambiae complex. 3619:246–274.

719 Coluzzi M, Sabatini A, Petrarca V, Di Deco M. 1979. Chromosomal differentiation
720 and adaptation to human environments in the Anopheles gambiae complex.
721 Trans R Soc Trop Med Hyg 73:483–497.

722 Coluzzi M, Sabatini A, Torre A, Angela M, Deco D, Petrarca V. 2002. A Polytene
723 Chromosome Analysis of the Anopheles gambiae Species Complex.
724 Science (80-.). 298:1415–1419.

725 Dabiré RK, Namountougou M, Sawadogo SP, Yaro LB, Toé HK, Ouari A,
726 Gouagna L-C, Simard F, Chandre F, Baldet T, et al. 2012. Population
727 dynamics of Anopheles gambiae s.l. in Bobo-Dioulasso city : bionomics,
728 infection rate and susceptibility to insecticides. Parasit. Vectors 5:127.

729 David J, Ismail HM, Chandor-proust A, Ingraham MJ, John M, Paine I. 2013.
730 Role of cytochrome P450s in insecticide resistance : impact on the control of

731 mosquito-borne diseases and use of insecticides on Earth Role of
732 cytochrome P450s in insecticide resistance : impact on the control of
733 mosquito-borne diseases and use of insecti. Philos. Trans. R. Soc. Lond. B.
734 Biol. Sci.

735 Davidson G. 1964. The five mating types of the Anopheles gambiae complex.
736 Riv. Malariol. 13:167–183.

737 Derua Y a, Alifrangis M, Hosea KM, Meyrowitsch DW, Magesa SM, Pedersen
738 EM, Simonsen PE. 2012. Change in composition of the Anopheles gambiae
739 complex and its possible implications for the transmission of malaria and
740 lymphatic filariasis in north-eastern Tanzania. Malar. J. 11:188.

741 Dia I, Guelbeogo M, Ayala D. 2013. Advances and Perspectives in the Study of
742 the Malaria Mosquito Anopheles funestus.

743 Enayati AA, Ranson H, Hemingway J. 2005. Insect glutathione transferases and
744 insecticide resistance. Insect Mol. Biol. 14:3–8.

745 Etang J, Nwane P, Mbida JA, Piameu M, Manga B, Souop D, Awono-Ambene P,
746 Ahmed AM, Braimah N, Drakeley C, et al. 2011. Variations of insecticide
747 residual bio-efficacy on different types of walls: results from a community-
748 based trial in south Cameroon. Malar. J. 10:333.

749 Excoffier L, Smouse PE, Quattro JM. 1992. Analysis of molecular variance
750 inferred from metric distances among DNA haplotypes: Application to human
751 mitochondrial DNA restriction data. Genetics 131:479–491.

752 Fanello C, Santolamazza F, DellaTorre A. 2002. Simultaneous identification of

753 species and molecular forms of the Anopheles gambiae complex by PCR-
754 RFLP. Med. Vet. Entomol. 16:461–464.

755 Fontaine MC, Pease JB, Steele a., Waterhouse RM, Neafsey DE, Sharakhov I
756 V., Jiang X, Hall a. B, Catteruccia F, Kakani E, et al. 2015. Extensive
757 introgression in a malaria vector species complex revealed by
758 phylogenomics. Science (80-.). 347:1258524–1258524.

759 Fossog Tene B, Poupardin R, Costantini C, Awono-Ambene P, Wondji CS,
760 Ranson H, Antonio-Nkondjio C. 2013. Resistance to DDT in an Urban
761 Setting: Common Mechanisms Implicated in Both M and S Forms of
762 Anopheles gambiae in the City of Yaoundé Cameroon. PLoS One 8.

763 Fouet C, Gray E, Besansky NJ, Costantini C. 2012. Adaptation to aridity in the
764 malaria mosquito Anopheles gambiae: chromosomal inversion
765 polymorphism and body size influence resistance to desiccation. PLoS One
766 7:e34841.

767 Fumagalli M, Vieira FG, Linderoth T. 2014. ngsTools : methods for population
768 genetics analyses from Next-Generation Sequencing data. Bioinformatics.

769 Georghiou GP. 1972. The evolution of resistance to pesticides. Annu. Rev. Ecol.
770 Syst. 3:133–168.

771 Gillies MT, Coetzee M. 1987. A supplement to the Anophelinae of Africa south of
772 the Sahara. Johannesburg: The South African Institute for Medical Research

773 Gillies MT, De Meillon B. 1968. The Anophelinae of Africa South of the Sahara.
774 Second Edi. Johannesburg: Publications of the South African Institute for

775 Medical Research

776 Hemingway J, Ranson H, Magill A, Kolaczinski J, Fornadel C, Gimnig J, Coetzee
777 M, Simard F, Roch DK, Hinzoumbe CK, et al. 2016. Averting a malaria
778 disaster: Will insecticide resistance derail malaria control? Lancet 387:1785–
779 1788.

780 Hendry AP, Gotanda KM, Svensson EI. 2017. Human influences on evolution,
781 and the ecological a nd societal consequences.

782 Huang DW, Sherman BT, Lempicki RA. 2009. Systematic and integrative
783 analysis of large gene lists using DAVID bioinformatics resources. Nat.
784 Protoc 4:44–57.

785 Irwin DE, Alcaide M, Delmore KE, Irwin JH, Owens GL. 2016. Recurrent
786 selection explains genomic regions of high relative but low absolute
787 differentiation in the greenish warbler ring species. Mol. Ecol. 25:4488–4507.

788 Jakobsson M, Rosenberg N. 2007. CLUMPP: a cluster matching and
789 permutation program for dealing with multimodality in analysis of population
790 structure. Bioinformatics 23:1801– 1806.

791 Jombart T. 2008. adegenet: a R package for the multivariate analysis of genetic
792 markers. Bioinformatics 24:1403–1405.

793 Jones CM, Toé HK, Sanou A, Namountougou M, Hughes A, Diabaté A, Dabiré
794 R, Simard F, Ranson H. 2012. Additional Selection for Insecticide
795 Resistance in Urban Malaria Vectors: DDT Resistance in Anopheles
796 arabiensis from Bobo-Dioulasso, Burkina Faso. PLoS One 7:e45995.

797 Kamdem C, Tene Fossog B, Simard F, Etouna J, Ndo C, Kengne P, Boussès P,
798 Etoa F-X, Awono-Ambene P, Fontenille D, et al. 2012. Anthropogenic
799 Habitat Disturbance and Ecological Divergence between Incipient Species of
800 the Malaria Mosquito Anopheles gambiae. PLoS One 7:e39453.

801 Korneliussen T, Albrechtsen A, Nielsen R. 2014. ANGSD: Analysis of Next
802 Generation Sequencing Data. BMC Bioinformatics 15:356.

803 Lawniczak MKN, Emrich SJ, Holloway a K, Regier a P, Olson M, White B,
804 Redmond S, Fulton L, Appelbaum E, Godfrey J, et al. 2010. Widespread
805 divergence between incipient Anopheles gambiae species revealed by
806 whole genome sequences. Science 330:512–514.

807 Lee Y, Marsden CD, Norris LC, Collier TC, Main BJ, Fofana A, Cornel AJ,
808 Lanzaro GC. 2013. Spatiotemporal dynamics of gene flow and hybrid fitness
809 between the M and S forms of the malaria mosquito, Anopheles gambiae.
810 Proc. Natl. Acad. Sci. U. S. A. 110:19854–19859.

811 Lenormand T, Bourguet D, Guillemaud T, Raymond M. 1999. Tracking the
812 evolution of insecticide resistance in the mosquito Culex pipiens. Nature
813 400:861–864.

814 Main BJ, Lee Y, Ferguson HM, Kreppel KS, Kihonda A, Govella NJ, Collier TC,
815 Cornel AJ, Eskin E, Kang EY, et al. 2016. The Genetic Basis of Host
816 Preference and Resting Behavior in the Major African Malaria Vector,
817 Anopheles arabiensis. PLoS Genet. 12:1–17.

818 Mallet J. 1989. The evolution of insecticide resistance: Have the insects won?

819 Trends Ecol. Evol. 4:336–340.

820 Maynard Smith J, Haigh J. 1974. The hitch-hiking effect of a favorable gene.
821 Genet Res 23:22–35.

822 Meirmans P, Van Tienderen P. 2004. GENOTYPE and GENODIVE: two
823 programs for the analysis of genetic diversity of asexual organisms. Mol.
824 Ecol. Notes 4:792–794.

825 Moiroux N, Gomez MB, Pennetier C, Elanga E, Djènontin A, Chandre F, Djègbé
826 I, Guis H, Corbel V. 2012. Changes in anopheles funestus biting behavior
827 following universal coverage of long-lasting insecticidal nets in benin. J.
828 Infect. Dis. 206:1622–1629.

829 Molineaux L, Gramiccia G. 1980. The Garki Project. Research on the
830 epidemiology and control of malaria in the sudan savanna of West Africa.
831 World Health Organization

832 Mourou J-R, Coffinet T, Jarjaval F, Pradines B, Amalvict R, Rogier C, Kombila M,
833 Pagès F. 2010. Malaria transmission and insecticide resistance of
834 Anopheles gambiae in Libreville and Port-Gentil, Gabon. Malar. J. 9:321.

835 Mwangangi JM, Mbogo CM, Orindi BO, Muturi EJ, Midega JT, Nzovu J, Gatakaa
836 H, Githure J, Borgemeister C, Keating J, et al. 2013. Shifts in malaria vector
837 species composition and transmission dynamics along the Kenyan coast
838 over the past 20 years. Malar. J. 12:13.

839 Ndjemaï HNM, Patchoké S, Atangana J, Etang J, Simard F, Bilong CFB, Reimer
840 L, Cornel A, Lanzaro GC, Fondjo E. 2009. The distribution of insecticide

841 resistance in Anopheles gambiae s.l. populations from Cameroon: an
842 update. Trans. R. Soc. Trop. Med. Hyg. 103:1127–1138.

843 Neafsey DE, Lawniczak MKN, Park DJ, Redmond SN, Coulibaly MB, Traoré SF,
844 Sagnon N, Costantini C, Johnson C, Wiegand RC, et al. 2010. SNP
845 genotyping defines complex gene-flow boundaries among African malaria
846 vector mosquitoes. Science 330:514–517.

847 Norris LC, Main BJ, Lee Y, Collier TC, Fofana A, Cornel AJ, Lanzaro GC. 2015.
848 Adaptive introgression in an African malaria mosquito coincident with the
849 increased usage of insecticide-treated bed nets. Proc. Natl. Acad.
850 Sci.:201418892.

851 Nosil P, Feder JL. 2012. Widespread yet heterogeneous genomic divergence.
852 Mol. Ecol. 21:2829–2832.

853 Nwane P, Etang J, Chouaïbou M, Toto J, Mimpfoundi R, Simard F. 2011. Kdr-
854 based insecticide resistance in Anopheles gambiae s.s populations in. BMC
855 Res. Notes 4:463.

856 Nwane P, Etang J, Chouaïbou M, Toto JC, Koffi A, Mimpfoundi R, Simard F.
857 2013. Multiple insecticide resistance mechanisms in Anopheles gambiae s.l.
858 populations from Cameroon, Central Africa. Parasit. Vectors 6:41.

859 O'Loughlin SM, Magesa S, Mbogo C, Mosha F, Midega J, Lomas S, Burt A.
860 2014. Genomic Analyses of Three Malaria Vectors Reveals Extensive
861 Shared Polymorphism but Contrasting Population Histories. Mol. Biol.
862 Evol.:1–14.

863 Oyewole IO, Awolola TS. 2006. Impact of urbanisation on bionomics and
864 distribution of malaria vectors in Lagos, southwestern Nigeria. J. Vector
865 Borne Dis. 43:173–178.

866 Palumbi SR. 2001. Evolution - Humans as the world's greatest
867 evolutionary force. Science (80-.). 293:1786–1790.

868 Paradis E, Claude J, Strimmer K. 2004. Analyses of Phylogenetics and Evolution
869 in R language. Bioinformatics 20:289–290.

870 Peterson BK, Weber JN, Kay EH, Fisher HS, Hoekstra HE. 2012. Double Digest
871 RADseq: An Inexpensive Method for De Novo SNP Discovery and
872 Genotyping in Model and Non-Model Species. PLoS One 7:e37135.

873 Pinto J, Egyir-Yawson A, Vicente J, Gomes B, Santolamazza F, Moreno M,
874 Charlwood J, Simard F, Elissa N, Weetman D, et al. 2013. Geographic
875 population structure of the African malaria vector Anopheles gambiae
876 suggests a role for the forest-savannah biome transition as a barrier to gene
877 flow. Evol. Appl. 6:910–924.

878 Purcell S, Neale B, Todd-Brown K, Thomas L, Ferreira M, Bender D, Maller J,
879 Sklar P, de Bakker P, Daly M, et al. 2007. PLINK: a toolset for whole-
880 genome association and population-based linkage analysis. Am. J. Hum.
881 Genet. 81.

882 R Development Core Team. 2014. R: A language and environment for statistical
883 computing. R Foundation for Statistical Computing, Vienna, Austria

884 Raj A, Stephens M, Pritchard JK. 2014. FastSTRUCTURE: Variational inference

885 of population structure in large SNP data sets. Genetics 197:573–589.

886 Ranson H, Lissenden N. 2016. Insecticide Resistance in African Anopheles
887 Mosquitoes: A Worsening Situation that Needs Urgent Action to Maintain
888 Malaria Control. Trends Parasitol. 32:187–196.

889 Reid MC, McKenzie FE. 2016. The contribution of agricultural insecticide use to
890 increasing insecticide resistance in African malaria vectors. Malar. J. 15:107.

891 Riehle MM, Guelbeogo WM, Gneme A, Eiglmeier K, Holm I, Bischoff E, Garnier
892 T, Snyder GM, Li X, Markianos K, et al. 2011. A cryptic subgroup of
893 Anopheles gambiae is highly susceptible to human malaria parasites.
894 Science 331:596–598.

895 Rosenberg N. 2004. DISTRUCT: a program for the graphical display of
896 population structure. Mol. Ecol. Resour. 4:137–138.

897 Santolamazza F, Torre A Della, Caccone A. 2004. Short Report : a New
898 Polymerase Chain Reaction − Restriction Fragment Length Polymorphism
899 Method To Identify Anopheles Arabiensis From an . Gambiae and Its Two
900 Molecular Forms From Degraded Dna Templates or Museum Samples.
901 Trop. Med. 70:604–606.

902 Savolainen O, Lascoux M, Merilä J. 2013. Ecological genomics of local
903 adaptation. Nat. Rev. Genet. 14:807–820.

904 Service MW. 1993. Mosquito ecology: field sampling methods. (Elsevier Applied
905 Science, London UK, editor.).

906 Silvestrini F, Severini C, di Pardo V, Romi R, de Matthaeis E, Raymond M. 1998.

907 Population structure and dynamics of insecticide resistance genes in Culex
908 pipiens populations from Italy. Heridity 81:342–348.

909 Simard F, Ayala D, Kamdem GC, Pombi M, Etouna J, Ose K, Fotsing J-M,
910 Fontenille D, Besansky NJ, Costantini C. 2009. Ecological niche partitioning
911 between Anopheles gambiae molecular forms in Cameroon: the ecological
912 side of speciation. BMC Ecol. 9:17.

913 Sinka ME, Bangs MJ, Manguin S, Coetzee M, Mbogo CM, Hemingway J, Patil
914 AP, Temperley WH, Gething PW, Kabaria CW, et al. 2010. The dominant
915 Anopheles vectors of human malaria in Africa, Europe and the Middle East:
916 occurrence data, distribution maps and bionomic précis. Parasit. Vectors
917 3:117.

918 Slotman M a, Tripet F, Cornel a J, Meneses CR, Lee Y, Reimer LJ, Thiemann
919 TC, Fondjo E, Fofana a, Traoré SF, et al. 2007. Evidence for subdivision
920 within the M molecular form of Anopheles gambiae. Mol. Ecol. 16:639–649.

921 Sogoba N, Vounatsou P, Bagayoko MM, Doumbia S, Dolo G, Gosoniu L, Traoré
922 SF, Smith T a, Touré YT. 2008. Spatial distribution of the chromosomal
923 forms of anopheles gambiae in Mali. Malar. J. 7:205.

924 Sokhna C, Ndiath MO, Rogier C. 2013. The changes in mosquito vector
925 behaviour and the emerging resistance to insecticides will challenge the
926 decline of malaria. Clin. Microbiol. Infect. 19:902–907.

927 Stephens M, Scheet P. 2005. Accounting for decay of linkage disequilibrium in
928 haplotype inference and missing-data imputation. Am. J. Hum. Genet.

929 76:449–462.

930 Stephens M, Smith NJ, Donnelly P. 2001. A new statistical method for haplotype
931 reconstruction from population data. Am. J. Hum. Genet. 68:978–989.

932 Storz JF. 2005. Using genome scans of DNA polymorphism to infer adaptive
933 population divergence. Mol. Ecol. 14:671–688.

934 Tajima F. 1989. Statistical method for testing the neutral mutation hypothesis by
935 DNA polymorphism. Genetics 123:585–595.

936 Takken W, Verhulst NO. 2013. Host Preferences of Blood-Feeding Mosquitoes.
937 Annu. Rev. Entomol.:433–453.

938 Tene Fossog B, Antonio-Nkondjio C, Kengne P, Njiokou F, Besansky NJ,
939 Costantini C. 2013. Physiological correlates of ecological divergence along
940 an urbanization gradient: differential tolerance to ammonia among molecular
941 forms of the malaria mosquito Anopheles gambiae. BMC Ecol. 13:1.

942 Tene Fossog B, Ayala D, Acevedo P, Kengne P, Ngomo Abeso Mebuy I,
943 Makanga B, Magnus J, Awono-Ambene P, Njiokou F, Pombi M, et al. 2015.
944 Habitat segregation and ecological character displacement in cryptic African
945 malaria mosquitoes. Evol. Appl. 8:326–345.

946 Tiffin P, Ross-Ibarra J. 2014. Advances and limits of using population genetics to
947 understand local adaptation. Trends Ecol. Evol. 29:673–680.

948 Touré Y, Petrarca V, Traoré S, Coulibaly A, Maiga H, Sankaré O, Sow M, Di
949 Deco M, Coluzzi M. 1998. The distribution and inversion polymorphism of
950 chromosomally recognized taxa of the Anopheles gambiae complex in Mali,

West Africa. Parassitologia 40:477–511.

Turissini D, Gamez S, White BJ. 2014. Genome-Wide Patterns of Polymorphism in an Inbred Line of the African Malaria Mosquito Anopheles gambiae. Genome Biol. Evol. 6:3094–3104.

Wakeley J. 1996. The variance of pairwise nucleotide differences in two populations with migration. Theor. Popul. Biol. 49:39–57.

White B, Lawniczak M, Cheng C, Coulibaly MB, Wilson MD, Sagnon N, Costantini C, Simard F, Christophides GK, Besansky NJ. 2011. Adaptive divergence between incipient species of Anopheles gambiae increases resistance to Plasmodium. Proc. Natl. Acad. Sci. 108:244–249.

White GB. 1974. Anopheles gambiae complex and disease transmission in Africa. Trans R Soc Trop Med Hyg 68:278–298.

WHO. 2012. Global Plan for Insecticide Resistance Management in Malaria Vectors. :24.

WHO. 2013. World malaria report 2013.

Wondji C, Simard F, Fontenille D. 2002. Evidence for genetic differentiation between the molecular forms M and S within the Forest chromosomal form of *Anopheles gambiae* in an area of sympatry. Insect Mol. Biol. 11:11–19.

Wondji C, Simard F, Petrarca V. 2005. Species and populations of the Anopheles gambiae complex in Cameroon with special emphasis on chromosomal and molecular forms of Anopheles gambiae ss. J. Med. Entomol.

Wu TD, Nacu S. 2010. Fast and SNP-tolerant detection of complex variants and

973 splicing in short reads. Bioinformatics 26:873–881.

974

975

976 FIGURE LEGENDS

977 **Figure 1. *Anopheles gambiae* complex sibling species are genetically**
978 **distinct.** A) PCA B) NJ Tree, and C) fastSTRUCTURE analyses clearly separate
979 the four *An. gambiae* complex species that occur in Cameroon into discrete
980 genetic clusters. Additional subdivision below the species level is apparent within
981 *An. coluzzii* and *An. gambiae.* D) Species composition varies strongly between
982 eco-geographic regions. Sampling sites are denoted by black dots.

983

984 **Figure 2. *Anopheles gambiae* is divided into three subpopulations.** A) PCA,
985 B) NJ Tree, and C) fastSTRUCTURE analyses reveal subdivisions within *An.*
986 *gambiae.* We term the most abundant group *GAM1*, while a second small, but
987 widely distributed group, is termed *GAM2*. Finally, most individuals from the
988 village of Nkolondom are genetically distinct from other *An. gambiae* suggestive
989 of local adaptation.

990

991 **Figure 3. *Anopheles coluzzii* is divided into four subgroups.** A) PCA, NJ
992 Tree, and C) fastSTRUCTURE reveal major population structuring between *An.*
993 *coluzzii* from the northern Savannah eco-geographic region and *An. coluzzii* from
994 the southern three forested regions. Within the south, D) PCA, E) NJ Tree, and
995 F) fastSTRUCTURE analyses separate mosquitoes based on geographic origin,
996 although clustering is not fully discrete indicating a dynamic interplay between
997 local adaptation and migration.

998

999 **Figure 4. The genetic distance (F_{ST}) between populations show recent**
1000 **radiation within *An. gambiae* and *An. coluzzii* clades**. In an unrooted, F_{ST}-
1001 based NJ tree, *An. melas* is most distant from all other species, while *An.*
1002 *gambiae* and *An. coluzzii* are sister species. Southern populations of *An. coluzzii*
1003 are more closely related to each other than to the northern savannah population.
1004 In contrast to geographic distance, the Douala subpopulation is genetically closer
1005 to Yaoundé rather than Coastal mosquitoes. Within *An. gambiae*, a relatively
1006 deep split is present between *GAM2* and *GAM1*, while *Nkolondom* appears to
1007 have recently diverged from *GAM1*.
1008
1009 **Figure 5. Genome scans reveal footprints of global and local adaptation in**
1010 ***An. gambiae* subpopulations.** A-C) Diversity and Tajima's *D* are plotted for
1011 each of the three subpopulations. Brown asterisks denote windows above the
1012 99th percentile or below the 1st percentile of empirical distribution of Tajima's *D*.
1013 D-E) Both absolute (d_{xy}) and relative (F_{ST}) divergence between populations are
1014 plotted across 150-kb windows. Red asterisks indicate windows above the 99th
1015 percentile of empirical distribution of F_{ST}. In all populations, concordant dips in
1016 diversity and Tajima's *D* are evident near the pericentromeric region of 2L where
1017 the *para* sodium channel gene is located. Three other selective sweeps located
1018 on the X and 3R chromosomes are highlighted (grey boxes).
1019
1020 **Figure 6. Strong signatures of selection are centered on xenobiotic**
1021 **resistance loci in subpopulations of *An. coluzzii.*** A-H) Grey boxes highlight

1022 five selective sweeps characterized by extreme values of F_{ST} and Tajima's *D*. As
1023 in *An. gambiae*, sharp declines in diversity and allele frequency spectrum at the
1024 *para* sodium channel gene are present in all populations. A sweep encompassing
1025 a cluster of detoxification genes on 3R is sharpest in urban mosquitoes.
1026
1027 **Figure 7. Spatially varying selection between urban and coastal**
1028 **populations.** For each of the three southern *An. coluzzii* subpopulations, 80
1029 reconstructed haplotypes are visualized by color-coding 28 bi-allelic SNPs in the
1030 3R GSTE/CYP450 sweep either grey or white. A single invariant haplotype -- all
1031 grey SNPs -- is common in (A) Yaoundé, less so in (B) Douala, and very rare in
1032 (C) coastal populations. D-E) Similarly, in PCA and NJ Tree analysis of the same
1033 28 SNPs, coastal individuals (navy blue) are diffuse across genotypic space,
1034 while Yaoundé mosquitoes (purple) are tightly clustered. As expected, Douala
1035 (pink) exhibits an intermediate degree of variation. F) STRUCTURE analysis
1036 based solely on the 28 SNPs within the sweep shows clear distinctions between
1037 the three populations.
1038
1039

1040 SUPPLEMENTAL FIGURE LEGENDS

1041 **Figure S1.** Detailed map of sampling sites in Cameroon.

1042

1043 **Figure S2.** Bayesian information criterion was used to determine the most likely
1044 number of clusters/populations for A) all 941 samples, B) all *An. coluzzii*, C) *An.*
1045 *coluzzii* from the northern savannah, D) *An. arabiensis*, E) the 309 individuals
1046 used for genome scans F) all *An. gambiae*, G) southern *An. coluzzii*, and H) *An.*
1047 *melas.* BIC scores for 1 to 50 clusters are plotted. The lower the BIC score the
1048 better the model fits the observed genetic diversity.

1049

1050 **Figure S3.** Southern (pale pink) and northern populations (deep pink) of *An.*
1051 *coluzzii* are readily separated in PCA (top) and NJ trees (bottom) using SNPs
1052 exclusively from any of the five chromosomal arms.

1053

1054 **Figure S4.** No population substructure is detectable within northern *An. coluzzii*
1055 using PCA and NJ tree analysis.

1056

1057 **Figure S5.** Mean sequencing coverage per individual is plotted in 300kb non-
1058 overlapping windows across the genome. Only individuals used in the genome
1059 scans are included in the coverage calculation.

Figure 1.

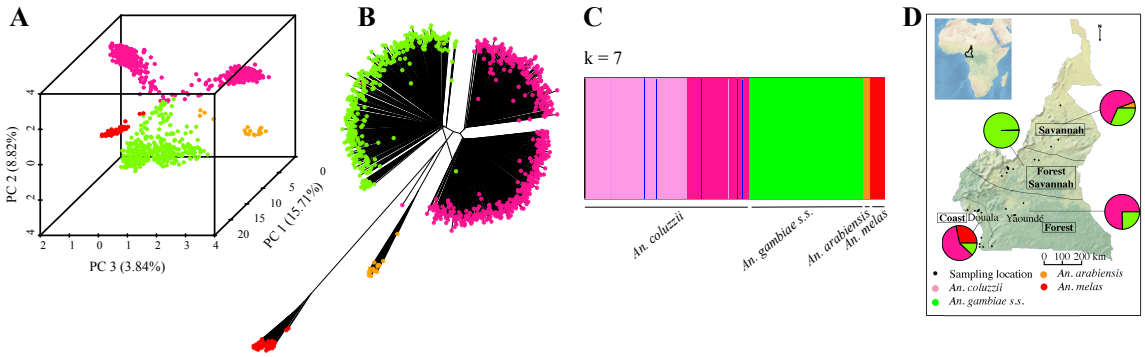
A
PC 2 (8.82%)
PC 3 (3.84%)
PC 1 (15.71%)
B
C
k = 7
An. coluzzii
An. gambiae s.s.
An. arabiensis
An. melas
D
Savannah
Forest Savannah
Coast
Douala
Yaoundé
Forest
0 100 200 km
Sampling location
An. coluzzii
An. gambiae s.s.
An. arabiensis
An. melas

Figure 2.

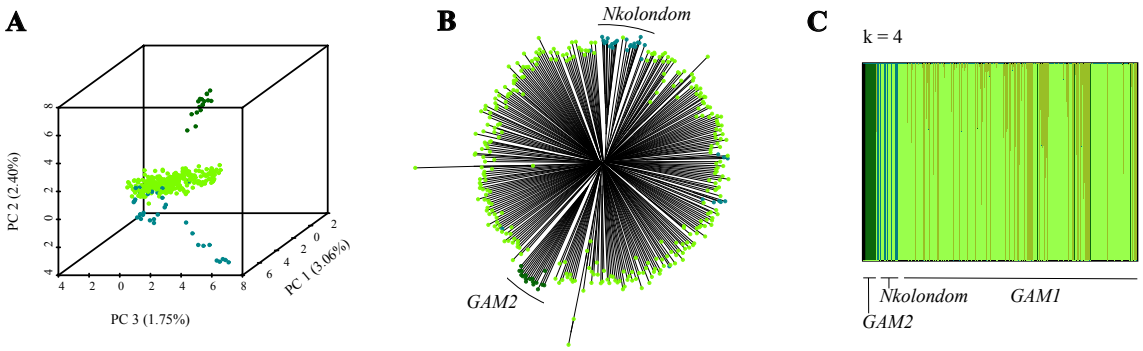
A
PC 2 (2.40%)
PC 3 (1.75%)
PC 1 (3.06%)
B
Nkolondom
GAM2
C
k = 4
Nkolondom
GAM1
GAM2

Figure 3.

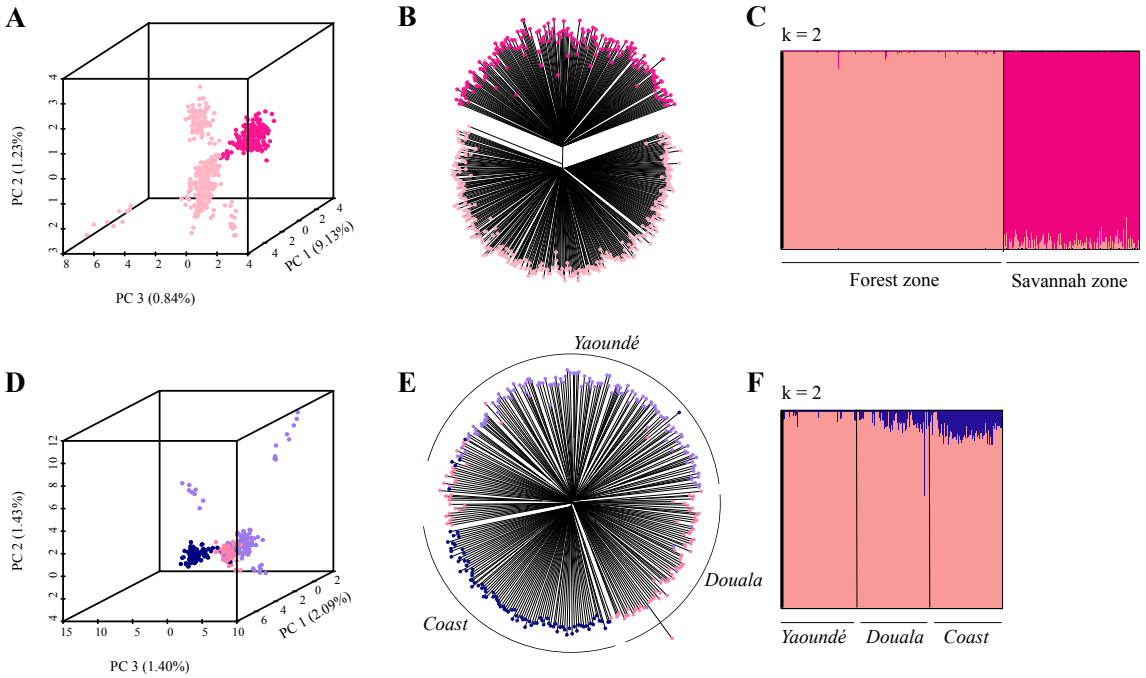
A
PC 2 (1.23%)
PC 3 (0.84%)
PC 1 (9.13%)
B
C
k = 2
Forest zone
Savannah zone
D
PC 2 (1.43%)
PC 3 (1.40%)
PC 1 (2.09%)
E
Yaoundé
Douala
Coast
F
k = 2
Yaoundé
Douala
Coast

Figure 4.

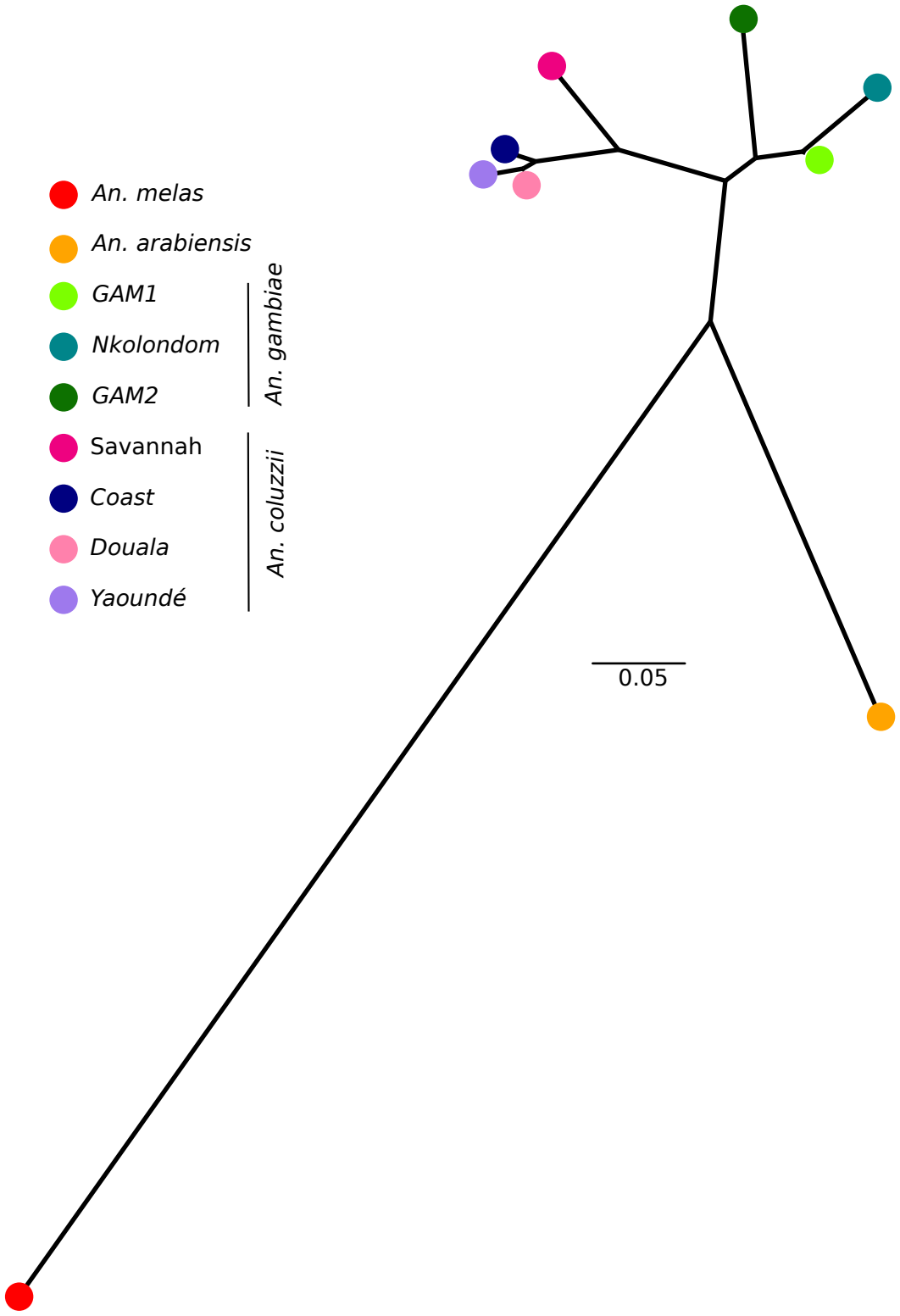
An. melas
An. arabiensis
GAM1
Nkolondom
GAM2
Savannah
Coast
Douala
Yaoundé
An. gambiae
An. coluzzii
0.05

Figure 5.

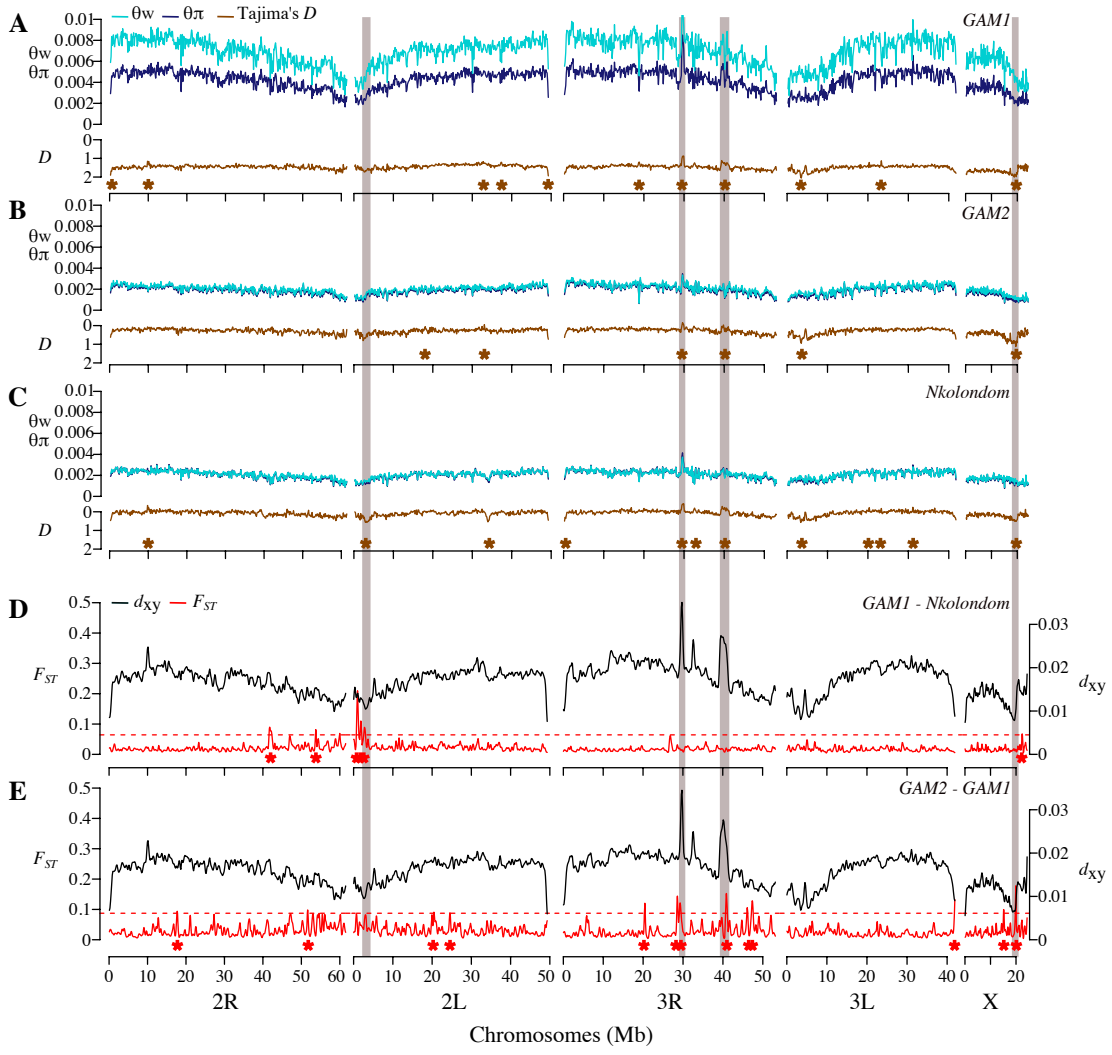
A
θw θπ Tajima's D
GAM1
B
GAM2
C
Nkolondom
D
dxy FST
GAM1 - Nkolondom
E
GAM2 - GAM1
2R
2L
3R
3L
X
Chromosomes (Mb)

Figure 6.

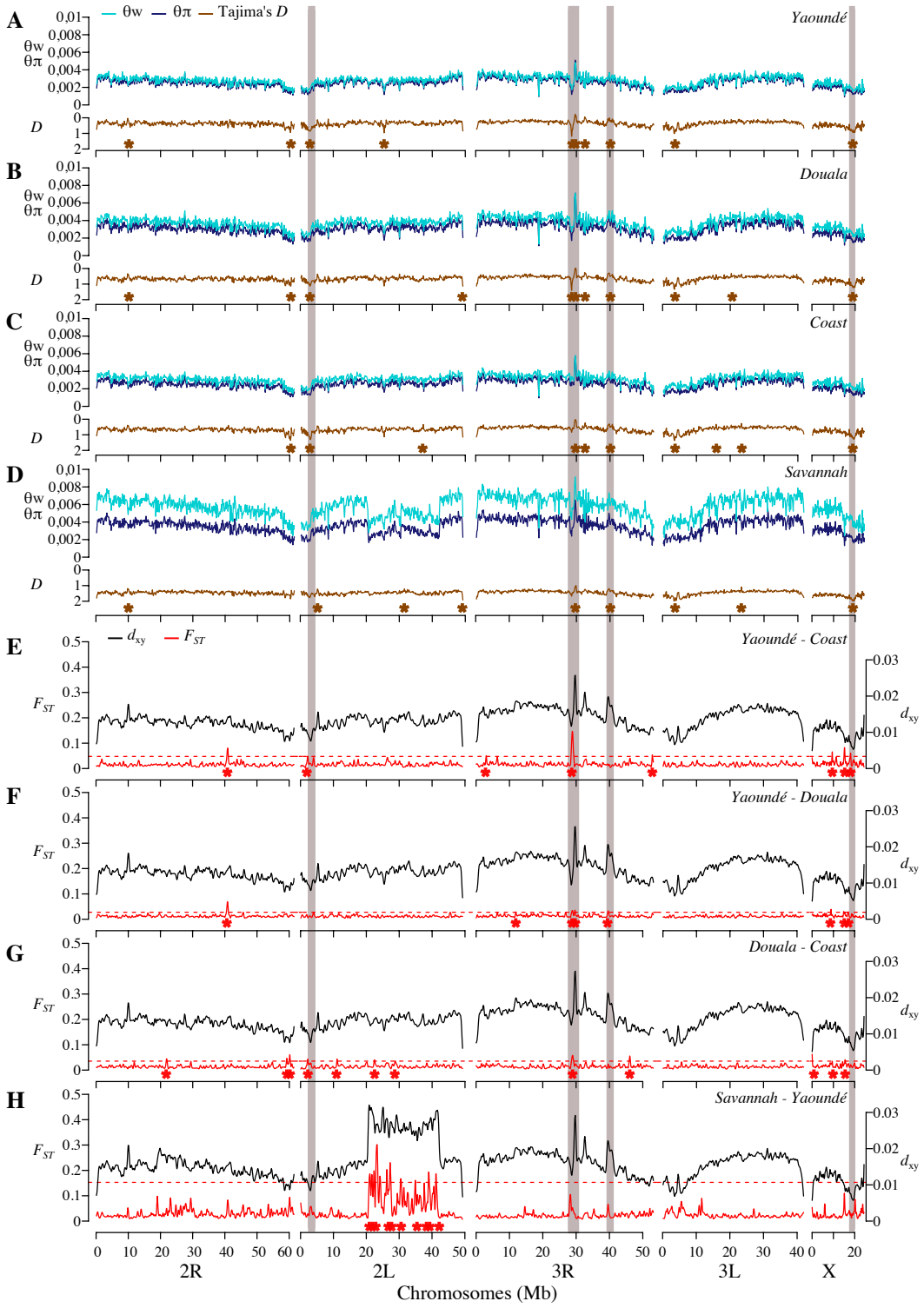
A
B
C
D
E
F
G
H
θw
θπ
Tajima's D
Yaoundé
Douala
Coast
Savannah
d_{xy}
F_{ST}
Yaoundé - Coast
Yaoundé - Douala
Douala - Coast
Savannah - Yaoundé
2R
2L
3R
3L
X
Chromosomes (Mb)

Figure 7.

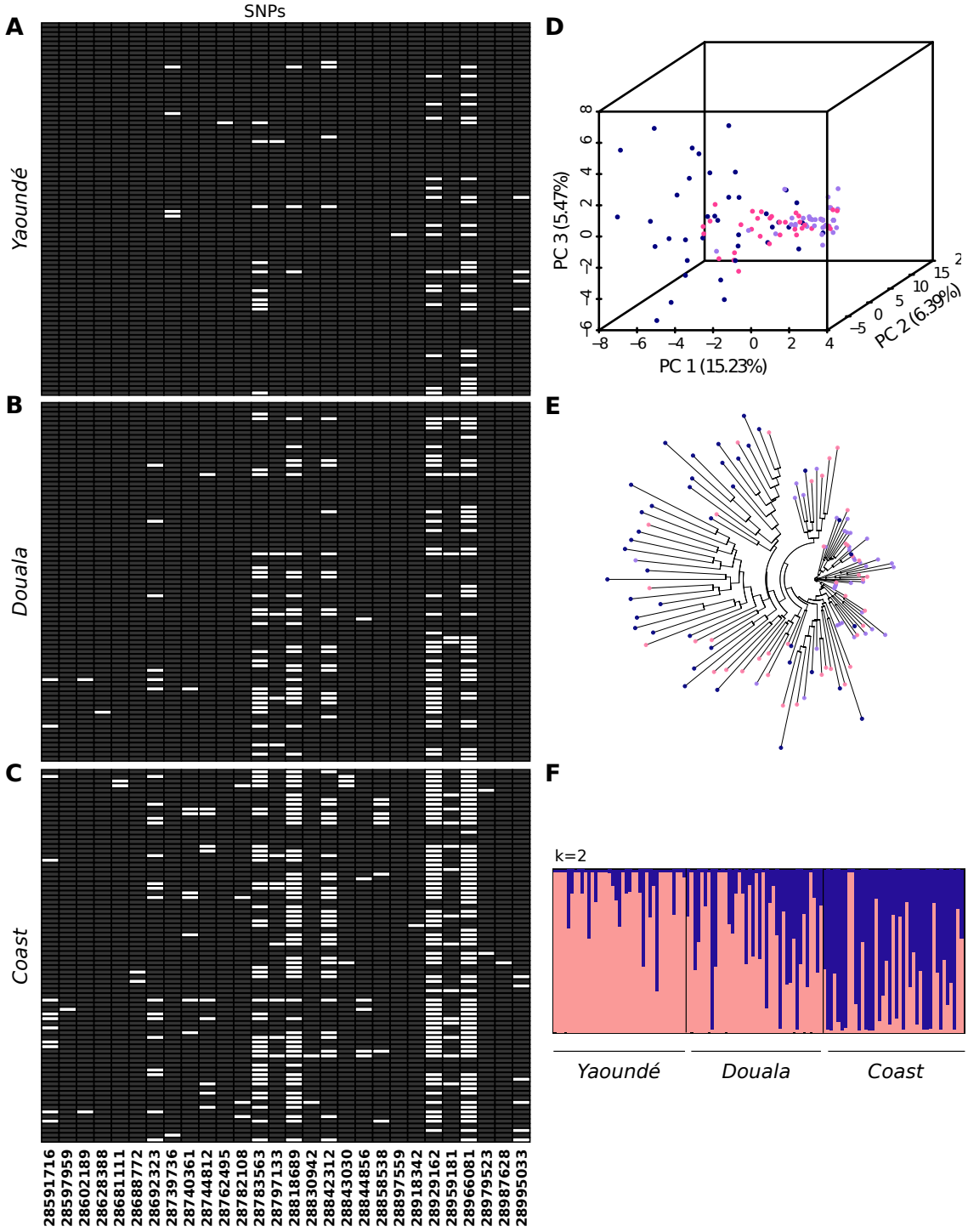
SNPs
A
Yaoundé
B
Douala
C
Coast
28591716
28597959
28602189
28628388
28681111
28688772
28692323
28739736
28740361
28744812
28762495
28782108
28783563
28797133
28818689
28830942
28842312
28843030
28844856
28858538
28897559
28918342
28929162
28959181
28966081
28979523
28987628
28995033
D
PC 3 (5.47%)
PC 1 (15.23%)
PC 2 (6.39%)
E
F
k=2
Yaoundé
Douala
Coast

Figure S1.

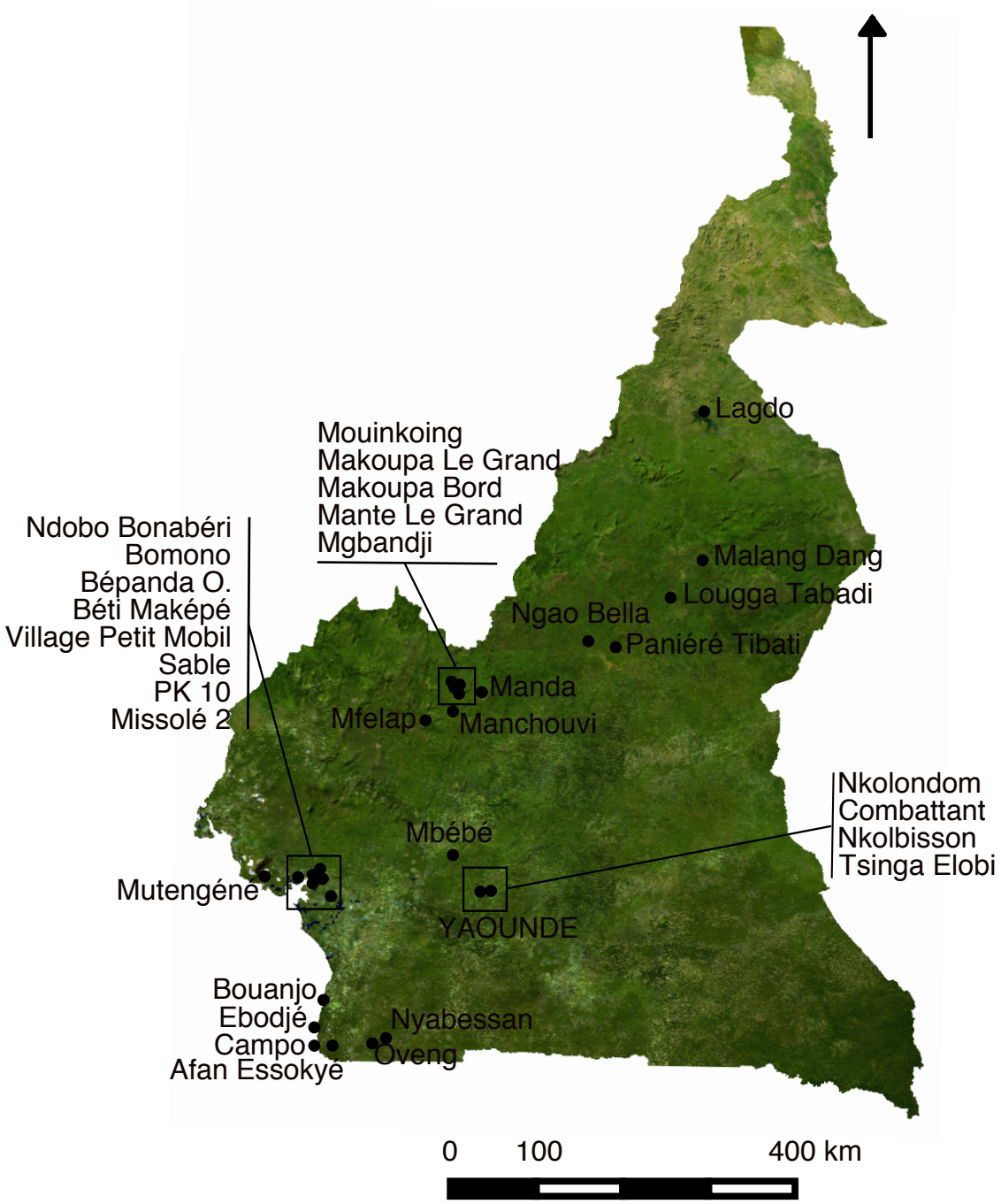
Lagdo
Mouinkoing
Makoupa Le Grand
Makoupa Bord
Mante Le Grand
Mgbandji
Ndobo Bonabéri
Bomono
Bépanda O.
Béti Maképé
Village Petit Mobil
Sable
PK 10
Missolé 2
Malang Dang
Lougga Tabadi
Ngao Bella
Paniéré Tibati
Manda
Mfelap
Manchouvi
Nkolondom
Combattant
Nkolbisson
Tsinga Elobi
Mbébé
Mutengéné
YAOUNDE
Bouanjo
Ebodjé
Campo
Afan Essokyé
Nyabessan
Oveng
0
100
400 km

Figure S2.

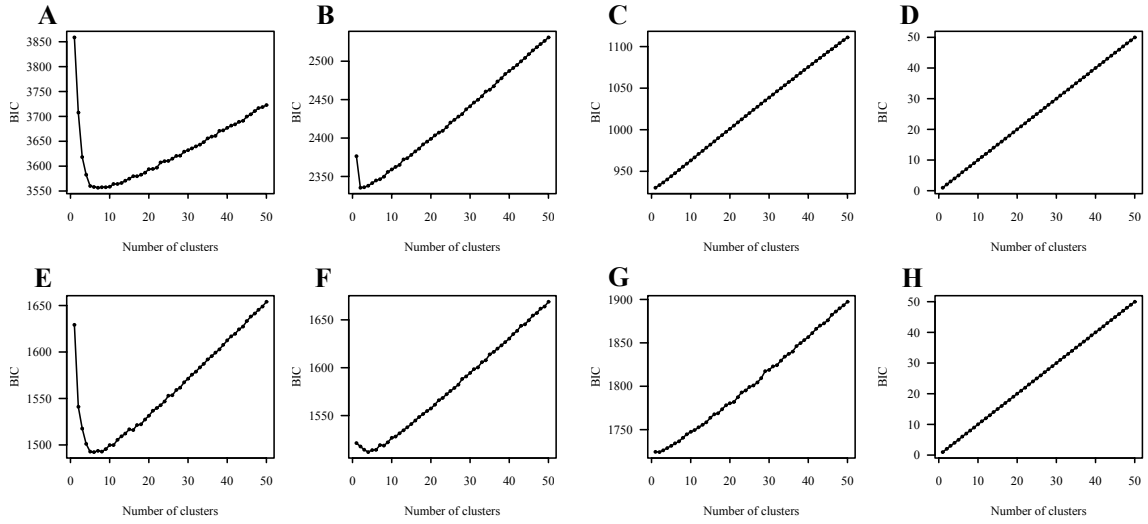

Figure S3.

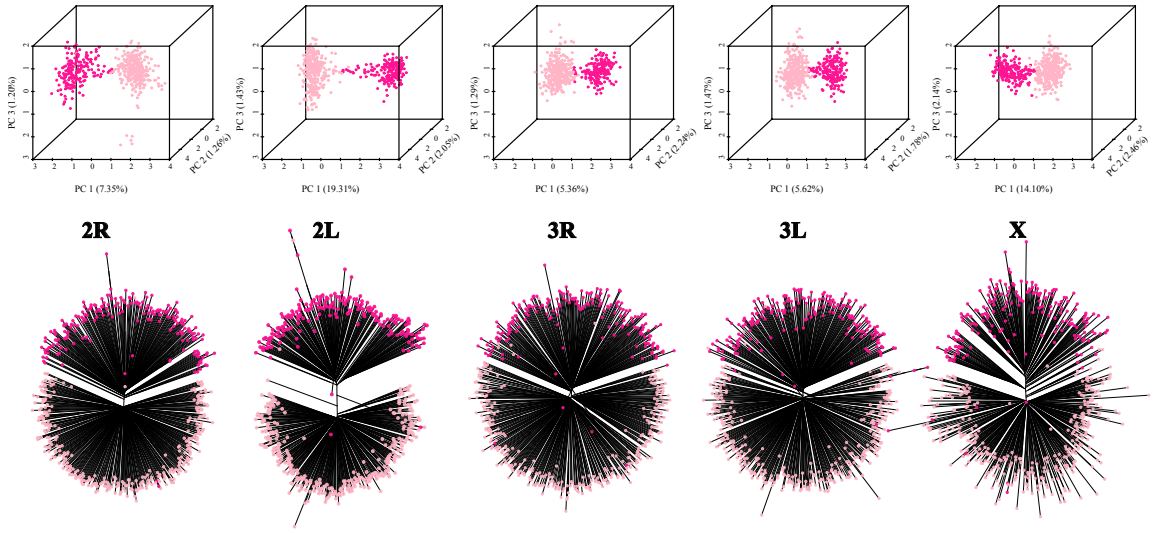
PC 1 (7.35%)
PC 2 (1.26%)
PC 3 (1.20%)
PC 1 (19.31%)
PC 2 (2.05%)
PC 3 (1.43%)
PC 1 (5.36%)
PC 2 (2.28%)
PC 3 (1.29%)
PC 1 (5.62%)
PC 2 (1.78%)
PC 3 (1.47%)
PC 1 (14.10%)
PC 2 (2.46%)
PC 3 (2.14%)
2R
2L
3R
3L
X

Figure S4.

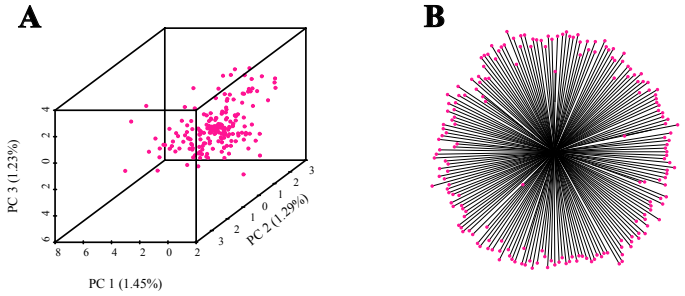

Figure S5.

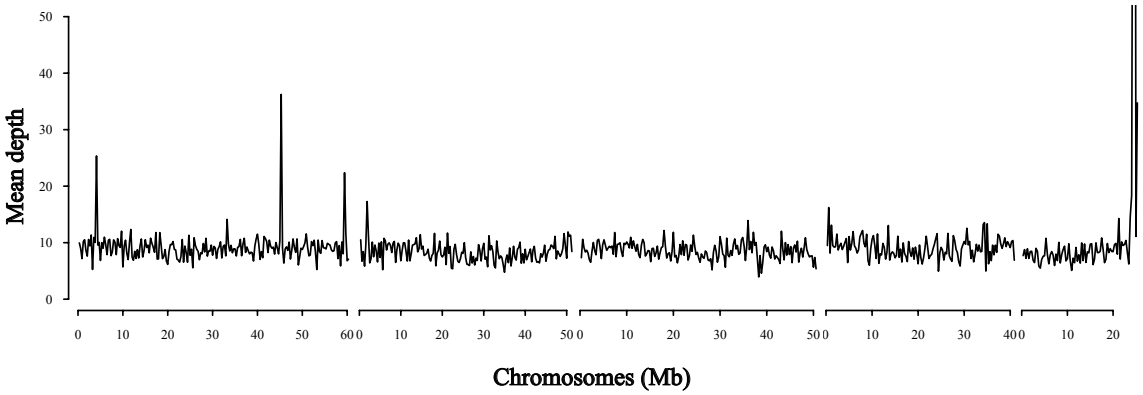

1060

1061

1062 SUPPLEMENTAL INFORMATION

1063 Consistently negative Tajima's *D* across all subgroups may reflect recent
1064 population expansions. To further address this hypothesis we modeled the
1065 demographic history of each population using a diffusion-based approach
1066 implemented in the software package ∂a∂i v 1.6.3 (Gutenkunst et al. 2009). We
1067 fit four alternative demographic models (*neutral, growth, two-epoch, bottle-*
1068 *growth*), without migration or recombination, to the folded allele frequency
1069 spectrum of each cryptic subgroup of *An. gambiae s.s.* and *An. coluzzii*. The best
1070 model was selected based on the highest composite log likelihood, the lowest
1071 Akaike Information Criterion (AIC), and visual inspection of residuals. As the
1072 choice of model can be challenging in recently diverged populations, we
1073 prioritized the simplest model when we found it difficult to discriminate between
1074 conflicting models. To obtain uncertainty estimates for the demographic
1075 parameters we used the built-in bootstrap function implemented in ∂a∂i to derive
1076 95% bootstrap confidence intervals.

1077 Results indicate that GAM1, GAM2, and Savannah populations have
1078 experienced recent size increases. However, for the southern populations of
1079 *Yaoundé, Coast, Douala, and Nkolondom* the best demographic model is a
1080 *bottle-growth* (Table S4). While most classical studies report *An. gambiae s.l.*
1081 populations that are in expansion (Donnelly et al. 2001), a more recent study
1082 employing RAD markers revealed that some East African populations have more
1083 complex demographic histories, often involving several changes in effective

1084 population size (N_e) as we observed in southern forest populations of both *An.*

1085 *coluzzii* and *An. gambiae* (O'Loughlin et al. 2014).

1086

1087 SUPPLEMENTAL REFERENCES

1088 Donnelly MJ, Licht MC, Lehmann T. 2001. Evidence for recent population
1089 expansion in the evolutionary history of the malaria vectors Anopheles
1090 arabiensis and Anopheles gambiae. Mol. Biol. Evol. 18:1353–1364.

1091 Gutenkunst RN, Hernandez RD, Williamson SH, Bustamante CD. 2009. Inferring
1092 the joint demographic history of multiple populations from multidimensional
1093 SNP frequency data. PLoS Genet. 5:e1000695.

1094 O'Loughlin SM, Magesa S, Mbogo C, Mosha F, Midega J, Lomas S, Burt A.
1095 2014. Genomic Analyses of Three Malaria Vectors Reveals Extensive
1096 Shared Polymorphism but Contrasting Population Histories. Mol. Biol.
1097 Evol.:1–14.

1098

Table S1. Locations of *An. gambiae s.l.* mosquitoes sequenced in Cameroon

Ecogeographic regions	Sampling locations	Geographic coordinates	Sampling methods				Total	*Anopheles gambiae sensu lato* populations identified								
			HLC-OUT	HLC-IN	LC	SPRAY		YDE	DLA	CST	SAV	GAM2	NKO	GAM1	A	ME
Savannah	Lagdo	9°02'56"N, 13°39'22"E	52	27	21	43	143				116			9	18	
	Lougga Tabadi	7°06'36"N, 13°12'36"E	2				2							2		
	Malang Dang	7°26'06"N, 13°33'14"E				11	11				2			9		
	Ngao Bella	6°30'04"N, 12°25'34"E	28	17		69	114				65	14		35		
	Paniéré Tibati	6°28'08"N, 12°37'44"E	5		22	16	43				13	1		29		
	Total		87	44	43	139	313				196	15		84	18	
Forest-Savannah Transition	Makoupa Bord	6°06'06"N, 11°11'29"E	2			16	18							18		
	Makoupa Le Grand	6°02'28"N, 11°10'39"E			4	10	14							14		
	Manchoutvi	5°52'48"N, 11°06'36"E			70		70					2		68		
	Manda	5°43'32"N, 10°52'06"E	1	2		33	36							36		
	Mante Le Grand	6°03'44"N, 11°12'18"E				8	8				1			7		
	Mfelap	5°43'30"N, 10°52'00"E				8	8							8		
	Mgbandji	6°05'49"N, 11°08'26"E			3	5	8							8		
	Mouinkoing	6°02'56"N, 11°24'36"E				3	3							3		
	Total		3	2	77	83	165				1	2		162		
Forest (urban)																
	Bepanda Omnisport (Doula)	4°03'18"N, 9°43'16"E			7		7		7							
	Beti Maképé (Douala)	4°03'54"N, 9°45'40"E			25		25		6					19		
	Bomono Gare (Douala)	4°04'55"N, 9°35'35"E			13		13		9					4		
	PK10 (Douala)	4°02'49"N, 9°46'47"E			20		20		16					4		
	Missolé 2 (Douala)	3°59'17"N, 9°54'22"E			8		8		8							
	Ndobo Bonabéri (Douala)	4°04'39"N, 9°40'12"E			1		1		1							
	Sable (Douala)	4°04'52"N, 9°43'34"E	28		5		33		33							
	Village Petit Mobil (Douala)	4°00'16"N, 9°45'18"E	1		16		17		17							
	Nkolbisson (Yaoundé)	3°52'29"N, 11°26'58"E			9		9	9								
	Nkolondom (Yaoundé)	3°58'20"N, 11°30'56"E			48		48	12					33	3		
	Tsinga Elobi (Yaoundé)	3°52'49"N, 11°30'23"E			46		46	46								
	Combattant (Yaoundé)	3°52'36"N, 11°30'46"E	18		48		66	65					1			
	Total		47	0	246	0	293	132	97				34	30		
Forest (rural)																
	Mbébé	4°10'00"N, 11°04'00"E				5	5							5		
	Nyabessan Centre	2°24'00"N, 10°24'00"E	4	1			5							5		
	Oveng	2°44'00"N, 11°27'00"E	1				1							1		
	Total		5	1	0	5	11							11		
Coast																
	Afan Essokyé	2°22'01"N, 9°58'59"E	1			13	14			3				11		
	Bouanjo	2°48'00"N, 9°54'00"E			5		5			5						
	Campo	2°22'01"N, 9°49'01"E	48		16	27	91			79				1		11
	Ebodjé	2°30'00"N, 9°49'05"E	35	4		3	42			5				3		34
	Mutengéné	4°06'53"N, 9°14'51"E			7		7		1	2				4		
	Total		84	4	28	43	159		1	94				19		45
Total			226	51	394	270	941	132	98	94	197	17	34	306	18	45

HLC-OUT, human landing catches performed outdoor; HLC-IN, human landing catches performed indoor; LC, larval collection; SPRAY, spray catches.

Table S2. Pairwise comparison of genetic distance (F_{ST}) among cryptic subgroups and sibling species of *An. gambiae s.l.*

F_{ST}	*Yaoundé*	*Douala*	*Coast*	*Savannah*	*GAM2*	*Nkolondom*	*GAM1*	*An. arabiensis*
Yaoundé	-							
Douala	0.016	-						
Coast	0.035	0.023	-					
Savannah	0.127	0.109	0.103	-				
GAM2	0.244	0.199	0.230	0.168	-			
Nkolondom	0.197	0.201	0.200	0.247	0.161	-		
GAM1	0.183	0.153	0.178	0.188	0.090	0.050	-	
An. arabiensis	0.451	0.406	0.498	0.383	0.478	0.372	0.327	-
An. melas	0.851	0.836	0.830	0.792	0.841	0.818	0.781	0.872

Table S3. Average nucleotide diversity in seven cryptic subgroups of *An. coluzzii* and *An. gambiae s.s*.

Population	θπ (bp^{-1})	θw (bp^{-1})
Yaoundé	0.0025	0.0028
Douala	0.0031	0.0037
Coast	0.0025	0.0031
Savannah	0.0035	0.0057
GAM2	0.0019	0.0020
Nkolondom	0.0020	0.0021
GAM1	0.0042	0.0069

Table S4. Parameters of demographic models inferred from folded Site Frequency Spectrum (SFS) of autosomal SNPs in seven cryptic subpopulations of *An. gambiae*

Species	Population	Best Model	Log Likelihood	Final Pop Size[a] (95% CI)	Bottleneck Size[b] (95% CI)	Time[c] (95% CI)
Anopheles coluzzii	*Yaoundé*	*Bottle-growth*	-83.45	1.18 (0.92 – 1.69)	24.85 (11.94 - 125.77)	0.58 (0.43 - 1.01)
	Douala	*Bottle-growth*	-84.50	2.20 (1.52 - 3.77)	5.66 (2.80 - 142.42)	0.59 (0.41 - 1.77)
	Coast	*Bottle-growth*	-82.95	1.72 (1.28 - 2.33)	23.83 (10.95 - 128.52)	0.67 (0.50 - 1.10)
Anopheles gambiae s.s.	*Savannah*	*Two-epoch*	-102.65	6.73 (6.35 - 7.21)		0.62 (0.54 - 0.72)
	GAM2	*Two-epoch*	-37.48	3.60 (1.74 - 7.70)		3.60 (0.56 - 9.30)
	Nkolodom	*Bottle-growth*	-74.92	1.08 (0.82 - 1.12)	24.95 (47.91 - 99.84)	0.63 (0.47 - 0.91)
	GAM1	*Two-epoch*	-103.33	6.75 (6.33 - 7.24)		0.68 (0.60 - 0.78)

[a] Ratio of contemporary to ancient population size.
[b] Ratio of population size after instantaneous change to ancient population size.
[c] Time in the past at which instantaneous change happened and growth began (in units of 2*Na generations).

Table S5. Functional analysis of gene ontology terms in candidate regions.
Supplementary online information